

UNIVERSIDADE DO VALE DO RIO DOS SINOS - UNISINOS
ESCOLA POLITÉCNICA
PROGRAMA DE PÓS-GRADUAÇÃO EM GEOLOGIA

ILANA LEHN

**FLUXOS GRAVITACIONAIS DE SEDIMENTOS: REGISTRO DE
TRANSFORMAÇÕES DE FLUXO NO RIFTE SANTA BÁRBARA OESTE, BACIA
DO CAMAQUÃ/RS**

São Leopoldo
2017

Ilana Lehn

FLUXOS GRAVITACIONAIS DE SEDIMENTOS: REGISTRO DE TRANSFORMAÇÕES
DE FLUXO NO RIFTE SANTA BÁRBARA OESTE, BACIA DO CAMAQUÃ/RS

Dissertação apresentada como requisito parcial
para a obtenção do título de Mestre em
Geologia, pelo Programa de Pós-Graduação
em Geologia, Universidade do Vale do Rio dos
Sinos - UNISINOS

Orientador: Prof. Dr. Paulo Sérgio Gomes Paim

Co-Orientador: Dr. Claus Fallgatter

Banca Avaliadora: Dr. Ernesto Luiz Correa Lavina

Dr. Renato Paes de Almeida

São Leopoldo

2017

L523f

Lehn, Ilana.

Fluxos gravitacionais de sedimentos : registro de transformações de fluxo no rifte Santa Bárbara Oeste, Bacia do Camaquã/RS / Ilana Lehn. – 2017.

/48 f. : il. ; 30 cm.

Dissertação (mestrado) – Universidade do Vale do Rio dos Sinos, Programa de Pós-Graduação em Geologia, 2017.

“Orientador: Prof. Dr. Paulo Sérgio Gomes Paim ; co-orientador: Dr. Claus Fallgatter.”

1. Turbiditos. 2. Debritos. 3. Camadas híbridas. 4. Transformações de fluxos. 5. Bacia do Camaquã. I. Título.

CDU 55

A dissertação de mestrado

**“FLUXOS GRAVITACIONAIS DE SEDIMENTOS: REGISTRO DE TRANSFORMAÇÕES DE FLUXO NO RIFTE
SANTA BÁRBARA OESTE, BACIA DO CAMAQUÃ/RS”**

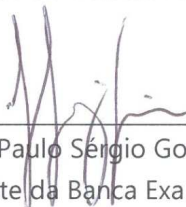
apresentada por **Ilana Lehn Fernandes**

foi aceita e aprovada como atendimento parcial aos requisitos para a obtenção do grau de

MESTRE EM GEOLOGIA pela seguinte banca examinadora:



Prof. Dr. Ernesto Luiz Corrêa Lavina
Universidade do Vale do Rio dos Sinos



Prof. Dr. Paulo Sérgio Gomes Paim
Presidente da Banca Examinadora
Universidade do Vale do Rio dos Sinos



Prof. Dr. Renato Paes de Almeida
Universidade de São Paulo
(Participação por webconferência) *

** Na presente sessão, fica o orientador autorizado a assinar pelo examinador que integra a banca via webconferência.*

São Leopoldo, 21 de fevereiro de 2017.

À minha mãe,
amor e exemplo supremos,
sempre a iluminar a vida.

AGRADECIMENTOS

À minha família, pelo amor e ensino constantes: minha mãe, Marisabel, toda a força que pode existir numa mulher, minha avó, Joveny, por toda uma vida de carinho e dedicação, meu avô, Hildomar (*in memoriam*), por me mostrar que a vida pode ser doce e ensolarada, minha irmã, Schana, minha zelosa jovem mãe, meu irmão, Christian, por permitir que eu babasse em seu peito, meus sobrinhos, Matheus e Arthur, dois grandes caras a continuar nossa história;

Ao meu parceiro (pra tudo e pra todas) Henrique Parisi Kern, pelas infindáveis horas de campo e discussão, entre uma cerveja e outra, e pelo abraço que sempre me consolou quando o mundo parecia ruir;

Ao meu orientador, Dr. Paulo Sérgio Gomes Paim, pelas geniais orientações, pela paciência diante dos meus erros e pelas piadinhas que salvavam os dias de revisões;

Aos meus parceiros de campo, Claus Fallgatter e Deise Silveira, por compartilharem os encantos e dúvidas mil que o Vale dos Lanceiros nos apresenta;

Aos amigos petrógrafos, Garibaldi Armelenti e Marinez Oliveira, por auxiliarem a olhar e tentar compreender um pequeno mundo que nos revela tanto;

A todos os professores do Programa de Pós-Graduação da UNISINOS, pelas discussões, troca de ideias e incansável transmissão de conhecimento. Agradecimento especial aos professores Dr. Farid Chemale Jr., Dra. Andrea Sander e Dra. Cassiana Michelin;

Ao Seu Manoel e bela família, pelo carinho sem igual na hospedagem na Segunda Capital Farroupilha, terra que aprendi a amar, Caçapava do Sul/RS;

Aos amigos, geólogos ou não, que estiveram em campo, bares e telefones, me dando apoio e ouvindo as lamúrias e dúvidas da geologia sedimentar;

Ao Universo, que permitiu minha vinda para esse planeta lindo para desvendar alguns dos mistérios que a Mãe-Terra nos proporciona;

Enfim, obrigada a todos que, de uma forma ou de outra, sorriram, torceram, me pagaram uma cerveja ou entoaram um “vai dar certo”!

“Tudo flui.”

Heráclito (535-475 a. C.)

SUMÁRIO

RESUMO EXPANDIDO	1
Resumo	1
Abstract.....	2
Introdução.....	2
Hipóteses e Objetivos	3
Métodos	4
Resultados.....	4
Considerações Finais	5
MANUSCRIPT	7
Abstract.....	7
1. Introduction	8
2. Geological Setting	9
3. Methods	13
4. Results	14
4.1 Facies and Facies Associations	14
4.2 Facies analyses	14
4.2.1 Massive sandstone – Sm.....	14
4.2.2 Trough-cross bedded sandstone - St.....	14
4.2.3 Undulated Sandstone - Su.....	15
4.2.4 Graded Sandstone to mudstone couplets - Sg	16
4.2.5 Inverse to Normal Graded Sandstone - Sin	16
4.2.6 Clayey sandstones - SC	16
4.2.7 Silty sandstone - SS	17
4.2.8 Mudstone - F.....	17
4.3 Microscopic Analyses	20
4.3.1 Petrography.....	20
5.3.2 X-Ray and Scanning Electron Microscopy	23

4.4 Facies Associations	25
4.4.1 Facies Association 1	25
4.4.2 Facies Association 2	26
4.4.3 Facies Association 3	26
4.5 Facies Tracts	28
4.5.1 Sequence Stratigraphy	28
4.5.1.1 Lowstand System Tract (LST)	29
4.5.1.2 Transgressive Systems Tract (TST)	31
4.5.1.3 Highstand System Tract (HST)	33
4.5.2 General Facies Tract	34
5. Discussion.....	35
6. Conclusions	41
7. Acknowledgements	42
8. References	42
SÍNTESE FINAL	47

FIGURE INDEX

Figure 1 – Geological map indicating the study area (red rectangle). The Cerro do Bugio and Santa Bárbara allogroups dip about 20° to ESE, except close the fault along the southeastern margin of the Western Santa Bárbara Rift (modified from CPRM (1995).	10
Figure 2 – Tectono-sedimentary evolution of the Camaquã Basin (after Paim <i>et al.</i> , 2014). .	11
Figure 3 – Correlation of the study area with previous columns proposed for the Camaquã Basin and Santa Bárbara interval.....	12
Figure 4 – Facies table. A) Massive sandstone with flame structure at the base; B) Amalgamated and truncated Su beds; C) Sin bed with alternation of lower and upper flow regime sedimentary structures and internal scours; D) Graded sandstone beds displaying upper flow regime plane bedding near the base and climbing ripple-cross lamination in the upper part of the beds; E) Trough-cross bedded sandstone bed with granules and mud clasts; F) Detail of a thin SC bed with dispersed coarse sand grains and granules; G) 3 cm thick SS bed; H) Mudstone-rich interval.	18
Figure 5 – Photomicrographs under polarized light illustrating composition and fabric of Sg facies. A) Sandstone composition; and B) partially fragmented mud clast and contorted,	

detrital mica grains. Volc=volcanic fragment, Plag=plagioclase, Met=metamorphic fragment, Q=quartz, K-feld=K-feldspar.	20
Figure 6 – Photomicrographs under polarized light showing sand grains (quartz, plagioclase and volcanic fragments) dispersed in a silty (A) and clayey (B) detrital matrix related to the SS and SC facies, respectively, Volc=volcanic fragment, Plag=plagioclase, Met=metamorphic fragment, Q=quartz, K-feld=K-feldspar.	21
Figure 7 – Mud clasts fragmentation (indicated by narrows) and mud incorporation into the matrix.	21
Figure 8 –Iron oxide cementation. A) Iron oxide coating (black arrows) and grains fillings (white double arrows); B) Quartz overgrowth (arrow). Note the original quartz shape delineated by thin iron oxide coating.	23
Figure 9 – Calcite cement highlighted by Alizarin Red. A) Calcite cement filling pores; B) High birefringence and relief calcite cement replacing lithic grains.	23
Figure 10 – X-ray diffraction graphics of proximal (left) and distal (right) debrites samples (SC facies). Notice that they present similar composition and include vermiculite in the matrix.	24
Figure 11 – SEM images of clay minerals. A) Contact between mud clast (left) and the clay mineral in the matrix (right); B) Zoom of the right zone of A) showing vermiculite crystals covered by microcrystalline, botryoidal quartz.	24
Figure 12 – SEM image and EDS graphic representation and related compositional table.	25
Figure 13 – Conceptual depositional model and facies tract, including proximal, intermediate and distal reaches of a delta front (facies association 1, 2 and 3, respectively). The A-A’ section shows the facies distribution along the delta front.	27
Figure 14 –Stratigraphic section extracted from image interpretation including log location, paleocurrent mean vectors, facies associations and key stratigraphic surfaces.	29
Figure 15 – Facies tracts demonstrated in three sedimentary logs described on delta front strata of the lowstand system tract. The logs are disposed from proximal (Log C), through intermediate (Log D) to distal (Log E) areas.	31
Figure 16 – Facies tracts demonstrated in sedimentary logs related to the transgressive system tract. Both logs acquired near the MFS. Log A represents proximal settings and Log B distal ones. The proportion of sand and mud is expressed on gamma ray graphics.	32
Figure 17 - Facies tracts demonstrated in three sedimentary logs acquired along the highstand system tract. The logs are disposed from the proximal (Log F) through intermediate (Log G) to distal (Log H) reaches.	34
Figure 18 – Changes on the mud clasts content along the delta front: lack and abundance of mud clasts in the St facies recorded in the proximal (A) and intermediate (B) portions of the delta front. Abundant mud clasts in the Sin (C) and Sg (D) facies present in the intermediate portions of the delta front; and E) low content of mud clasts in the distal, mud-rich portions of the delta front.	36

Figure 19 – Incorporation of clay into turbidite facies: erosion of a lower muddy layer producing mud clasts (A) that are progressively crushed (B) and turned into a clayey depositional matrix (C)..... 38

Figure 20 – Outcrop photograph in the studied area and graphic representation of hybrid bed; debrite on the base, sandy turbidite with ripple-cross lamination on top and thin mud cap (Modified from Talling *et al.*, 2012). 39

Figure 21 – Facies tract and flow evolution model. From 1 to 4: stream flow at the mouth bar, bipartite flow, high and low-concentration turbidity currents, mud incorporation and transformation into a debris flow and deposition of the turbidity plume derived from the dilution of the upper part of the debris flow. 40

RESUMO EXPANDIDO

FLUXOS GRAVITACIONAIS DE SEDIMENTOS: REGISTRO DE TRANSFORMAÇÕES DE FLUXO NO RIFTE SANTA BÁRBARA OESTE, BACIA DO CAMAQUÃ/RS

Ilana Lehn¹

¹ Universidade do Rio dos Sinos – UNISINOS

RESUMO

Fluxos gravitacionais de sedimentos compreendem correntes densas de fundo caracterizadas pela alta concentração de sedimentos. Declive abaixo, transformações de fluxo podem ocorrer (fluxo laminar para turbulento e *vice-versa*) devido a diversos fatores, inclusive à incorporação de argila ou segregação da mesma no fluxo. Transformações de fluxo podem causar comportamentos híbridos de fluxo, quando um mesmo fluxo apresenta mais de uma reologia e assim gera camadas com características híbridas. O Rifte Santa Bárbara Oeste, o qual representa um estágio evolutivo de natureza transtensional da Bacia do Camaquã (Rio Grande do Sul) inclui depósitos de fluxos gravitacionais de sedimentos coesivos (debritos) e não-coesivos (turbiditos). Esta pesquisa tem como objetivo testar a possível conexão genética entre os dois tipos de depósitos, entender o mecanismo de disparo destes fluxos e caracterizar as possíveis transformações de fluxo ocorridas ao longo do eixo deposicional da bacia. Análises fotoestratigráficas foram realizadas a fim de identificar superfícies estratigráficas-chave e tratos de sistemas associados. Perfis sedimentológicos e gama em escala de detalhe (1:20) e descrição pontual de afloramentos foram realizados a fim de identificar as fácies e associação de fácies na área de estudo. Durante estes trabalhos de campo, amostras foram coletadas para descrições macro e microscópicas. A associação de fácies sugere um contexto de frente deltaica caracterizado por fluxos unidirecionais para NE, paralelos ao eixo da bacia. O trato de fácies indica transformações de fluxo ocorridas desde a desembocadura dos distributários deltaicos. Na desembocadura ao ser desconfinado o fluxo sofre expansão e desacelera, gerando um intervalo denso no fundo de uma corrente de turbidez bipartida. Quando do congelamento friccional de seu intervalo laminar basal, a corrente de turbidez residual, totalmente turbulenta, e por isto com alta capacidade de erosão, erode o substrato, incorporando lama e gradualmente transformando-se em um fluxo de detritos. Por último, uma pluma em suspensão se desenvolve no topo do fluxo de detritos por diluição deste e gera uma delgada camada de turbidito no topo do debrito (camada híbrida).

Palavras-chave: Turbiditos, Debritos, Camadas Híbridas, Transformações de Fluxos, Bacia do Camaquã.

ABSTRACT

Sediment gravity flows comprise gravity-driven underflows characterized by a large concentration of suspended sediments. Along the downslope transport of sediments some flow transformations (laminar to turbulent flow and *vice versa*) can take place due to the incorporation or segregation of clay into or out the flow, respectively. These flow changes along a single depositional event indicating hybrid behavior and may produce deposits called hybrid events beds. The Western Santa Bárbara Rift (Camaquã Basin, Brazil) includes both cohesive (debrites) and non-cohesive (turbidites) gravity flow deposits. This research aims to test a possible connection between both types of deposits, to understand their triggering mechanisms and to characterize possible flow transformations taking place along their downslope evolution. A photostratigraphic analysis was performed to identify key stratigraphic surfaces and associated system tracts. Detailed sedimentological and gamma logs (scale 1:20) and outcrops description were performed to identify facies and facies association. During field campaigns, sampling was undertaken to provide material for microscopic (optical and SEM) and X-ray analyses. The stratigraphic record suggests a longitudinal, northeasterward delta system. Facies tract indicates several flow transformations taking place downslope from the distributary mouth bars. The suspended load at the streams mouths produces dense underflows that become bipartite as the flow decelerates and thins out. As soon as the denser interval of the bipartite current freezes, the upper, turbulent layer with high erosion capacity erodes the substrate, incorporates mud and gradually becomes a debris flow. At last a dilute plume develops along the upper layer of debris flows due to flow dilution and deposits a thin turbidite layer above the debrite as a hybrid bed.

Key-words: Turbidites, Debrites, Hybrid Beds, Santa Bárbara West Rift, Camaquã Basin.

INTRODUÇÃO

É amplamente reconhecida a importância de turbiditos como reservatórios de óleo e gás. Por outro lado, debritos geneticamente associados podem atuar como selantes ou barreiras de permeabilidade neste tipo de reservatório. Nos turbiditos aflorantes na área de trabalho é comum uma associação física entre turbiditos e debritos.

O intervalo de estudo mais geral compreende parte da Aloformação Serra dos Lanceiros (Paim *et al.*, 2000) e da Sequência 1 (Almeida, 2001) pertencentes ao Alogrupo e Grupo Santa Barbara, respectivamente. A Aloformação Serra dos Lanceiros registraria uma sequência deposicional única, limitada na base e no topo por discordâncias subaéreas, e composta por depósitos aluviais, fluviais entrelaçados, deltaicos e lacustres. Já a

Sequência 1 incluiria depósitos vinculados a sistemas aluviais, fluviais entrelaçados e marinhos (planícies de mares e estuários, incluindo deltas de cabeceira e baía central). Por similaridades genéricas nas interpretações, a concepção de Paim *et al* (2000) foi adotada e detalhada. A Aloformação Serra dos Lanceiros compreende parte do preenchimento superior do Rifte Santa Bárbara Oeste (Paim *et al.*, 2014). O intervalo escolhido para detalhamento sedimentológico sobre turbiditos e debritos com indícios de cogeneticidade compreende uma das sequências deposicionais discriminadas via fotoestratigrafia neste trabalho. Para este estudo, fácies sedimentares deltaicas representando desde porções proximais até distais da frente deltaica foram descritas e analisadas.

A escolha do Rifte Santa Bárbara Oeste é justificada pela exposição de uma espessa sucessão de fácies de origem fluvial e deltaica exposta em uma estrutura homoclinal. Deste modo, os estratos, bastante inclinados, expõem em vista aérea uma seção geológica completa passível de ser analisada via fotointerpretação de forma análoga a uma seção sísmica. Essa disposição estrutural favorece a contextualização lateral e vertical das fácies descritas, devido à continuidade de várias superfícies estratigráficas-chaves, permitindo assim melhor compreender as fácies em termos de mudanças *downdip* (trato de fácies) e verticais (tratos de sistemas).

HIPÓTESES E OBJETIVOS

A pesquisa parte da seguinte hipótese de trabalho: os depósitos associados a fluxos coesivos e não-coesivos são geneticamente associados e derivam originalmente de correntes hiperpicnais. Assim sendo, os objetivos do mestrado incluem (1): definir os mecanismos de transporte e a reologia dos fluxos a partir da caracterização macro e microscópica das fácies sedimentares; (2) caracterizar o trato de fácies no sentido *downdip* a partir da espacialização das fácies previamente descritas dentro de um arcabouço estratigráfico genético; e (3) a partir dos resultados destas duas escalas de trabalho qual seriam o mecanismo de ignição dos fluxos e as possíveis transformações que os mesmos sofriram ao longo de suas rotas bacía adentro.

MÉTODOS

Foi inicialmente realizada a fotointerpretação da área, com o uso de fotos aéreas na escala 1:25.000 e imagens do *software Google Earth*. Esta análise buscou reconhecer superfícies estratigráficas-chave, bem como identificar possíveis diferenças litológicas. A etapa seguinte compreendeu trabalho de campo, onde foram levantados perfis sedimentológicos e gama em escala de detalhe (1:20) e descritos pontos de controle a fim de averiguar as fácies que compunham as distintas litologias previamente reconhecidas em fotos aéreas. Nessa etapa também foram coletadas amostras das principais fácies. Foram descritas oito fácies sedimentares, a partir da composição, fábrica e estruturas sedimentares. Análises petrográficas, de difração de raio-X e de microscopia eletrônica de varredura (MEV) foram realizadas a fim de reconhecer a presença, tipo e distribuição de matriz argilosa nas amostras. As fácies sedimentares foram reunidas em três associações de fácies, dispostas em tratos de fácies. Essa distribuição *downdip* de fácies (trato de fácies) possibilitou a geração de um modelo de evolução e transformação de fluxo.

RESULTADOS

O reconhecimento e interpretação das fácies sedimentares em conjunto sugerem um contexto geral de frente deltaica. A disposição destas num trato de fácies levou à interpretação das transformações ocorridas nos fluxos durante seus percursos bacia adentro. Fácies arenosas encontram-se preservadas nas porções mais proximais da frente deltaica e representam barras sigmoidais depositadas quando do desconfinamento de fluxos canalizados e turbiditos arenosos gerados por correntes de turbidez alta concentração. A porção intermediária da frente deltaica apresenta predomínio de depósitos de turbiditos de baixa concentração e hiperpicnitos. Por fim, nas porções mais distais da frente deltaica, turbiditos de baixa concentração dividem espaço com depósitos de debritos, debritos arenosos, camadas híbridas e pelitos lacustres.

A disposição de fácies identificada possibilita o reconhecimento de três transformações de fluxo; (1) inicialmente, na foz de distributários de natureza entrezada, a carga em suspensão descola-se da carga de fundo, deixando para traz as camadas sigmoidais

estratificadas e gerando uma corrente de turbidez de natureza turbulenta. Esta sofre gradativa expansão e diminuição de velocidade e transforma-se gradualmente em uma corrente de turbidez bipartida (primeira transformação de fluxo - TF1); (2) o congelamento friccional do intervalo de alta concentração basal deixa para trás os turbiditos de alta concentração e libera uma corrente de turbulenta que acelera ao longo do talude deltaico, erodindo e incorporando lama do substrato, e gradativamente transformando-se em um fluxo laminar de detritos (TF2); e, por fim, (3) a incorporação de água na cabeça e porção superior do fluxo de detritos gera uma pluma diluída e turbulenta (TF3) que recobre e (camadas híbridas) e eventualmente ultrapassa os debritos.

CONSIDERAÇÕES FINAIS

O artigo submetido à revista *Sedimentary Geology* apresenta os principais resultados da pesquisa realizada durante o período do mestrado da proponente. Essa pesquisa focou depósitos de fluxos coesivos (debritos) e não coesivos (turbiditos) aflorantes no Rifte Santa Bárbara Oeste sob do ponto de vista de evolução do fluxo ao longo de sua trajetória.

Através da caracterização e análise de um trato de fácies contextualizado em um arcabouço estratigráfico genético foi proposto um modelo evolutivo para efluentes deltaicos fluindo ao longo de um talude deltaico. A carga sedimentar de efluentes derivados dos distributários deltaicos entrelaçados separam-se ao alcançar a foz de distributários. Primeiramente depositam corpos sigmoidais junto à foz (carga de fundo) enquanto sua carga em suspensão afunda e gera correntes de turbidez que gradualmente evoluem de turbulentas para bipartidas (TF 1). Enquanto o intervalo laminar basal de alta concentração congela a corrente residual, turbulenta e de baixa concentração, o suplanta e começa a incorporar lama de fundo até se transformar em fluxos de detritos (TF2). Estes, por fim, ao incorporarem água ao longo de sua trajetória, acabam por gerar um fluxo turbulento diluído em sua porção superior que deposita delgados turbiditos de baixa concentração acima dos debritos (camadas híbridas), podendo eventualmente ultrapassar os debritos depositando-se mais distalmente. Cabe que um talude deltaico de baixo gradiente formado em um lago raso e submetido a grandes flutuações de seu nível de base, propiciavam a dissecação de lama em ambiente de frente deltaica. A posterior

incorporação na forma de clastos de argila pelas correntes de turbidez turbulentas, que por ali fluíam, ocorria durante episódios de enxurradas e nível de lago alto.

Co-genetic, cohesive and non-cohesive delta front facies: a study case in the Camaquã Basin, southernmost Brazil

Ilana Lehn¹, Claus Fallgatter², Henrique Parisi Kern¹, Paulo Sérgio Gomes Paim¹

¹ Universidade do Vale do Rio dos Sinos – UNISINOS – São Leopoldo, RS. Brasil
E-mail: ilanalehn@gmail.com

² Department of Geology and Petroleum Geology - University of Aberdeen (UK)

ABSTRACT

Sediment gravity flows comprise gravity-driven underflows characterized by a large concentration of suspended sediments. Along the downslope transport some flow transformations (laminar to turbulent flow and vice-versa) can take place due to several factors, including the incorporation or segregation of clay into or from the flow, respectively. These flow changes produce hybrid behavior and resulting hybrid events beds. The Ediacaran Western Santa Bárbara Rift (Camaquã Basin) includes both cohesive (debrites) and non-cohesive (turbidites) gravity flow deposits. This research aims to test a possible connection between both types of deposits, to understand their triggering mechanisms and to characterize possible flow transformations taking place along the downslope route. As strata are dipping about 20° to SE, an aerial view of the area is comparable to a seismic section and allowed a downdip analysis of the entire succession. Therefore, a sequence stratigraphic approach was applied to identify on aerial photos and satellite images stratigraphic key surfaces and associated system tracts. Detailed sedimentological and gamma-ray logs (scale 1:20), outcrop descriptions, sampling, and thin section, X-ray diffraction and SEM analyses were performed to characterize and interpret facies and facies associations. The stratigraphic record registers a braidplain delta system with unidirectional flows to NE. Facies association 1 represents a proximal delta front context and contains sigmoidal, mouth bar deposits interfingered with high-concentration turbidites. Facies association 2 records the intermediate realm of the delta front where low-concentration turbidites dominate. At last, facies association 3 characterizes the distal portion of delta front where turbidites are interfingered with debrites and fine-grained, prodelta to lacustrine facies. Facies associations 1, 2 e 3 are stacked within the discriminated depositional sequences (facies successions) as well as distributed in the same way in the downdip direction (facies tract). Facies tract indicates a flow separation at the streams mouths, where sigmoidal bar are deposited and the suspended load bypasses as a turbulent underflow. Subsequent deceleration of the latter due to flow spreading produces bipartite turbidity currents (flow transformation 1) from which high-concentration turbidites are deposited due to frictional freezing. The residual, turbulent turbidity current accelerates along the delta slope, erodes the substrate, incorporates mud and gradually changes into a debris flow (flow transformation 2). A

diluted plume developed along the upper layer of the debris flow due to water incorporation characterizes the third flow transformation and produces a thin layer of turbidite at the top of almost each debrite (hybrid event bed).

Key-words: Turbidites, Debrites, Hybrid Beds, Delta System, Lacustrine Facies.

1. INTRODUCTION

Sediment gravity flows comprise sediment-fluid mixtures that flow downslope under the action of gravity (Middleton & Hampton, 1973). Sediment gravity flows could show fluid or plastic behavior, with corresponding flows termed fluidal and debris flows, respectively. Any flow may change its nature as a result of changes in sediment concentration along its downslope movement (Mulder and Alexander, 2001) and these flow transformations can be either from laminar (cohesive) to turbulent (non-cohesive) or *vice-versa*. The concept of flow transformation is useful to understand and visualize the flow dynamics in a sequential development of beds within single depositional units (Fisher, 1983). Beds that record the deposition “at a fixed point” of a non-cohesive and a cohesive flow behavior during the passage of a single sediment gravity flow are called hybrid beds (Haughton et al., 2009).

The study interval is part of the fill of the Ediacaran Camaquã Basin (southernmost Brazil) and belongs to the Serra dos Lanceiros Alloformation of Paim *et al.* (2000), Sequence 1 of Almeida (2001) and Arroio Umbu Formation of Justo & Almeida (2004). According to Paim et al. (2000), it comprises delta front sandstones and mudstones and prodelta to lacustrine mudstones. The delta front facies include mouth bar deposits, turbidites and debrites and lacustrine mudstones.

To understand the downdip changes on flow behavior from the geological record is a complex issue in not-well exposed basins with limited lateral extension, such as the case herein presented. However, due to the structural dip of the beds, flooding surfaces are apparent and correlation of outcrops and logs are easily performed through photointerpretation.

The delta deposits here presented show evidences of sediment gravity flows developed in shallow lacustrine settings. However, they differ in one or more aspect from other examples published elsewhere describing both deep-water (Ricci Lucchi *et al.*, 1980; Tinterri *et al.*, 2003; Talling *et al.*, 2004; Fonesu *et al.*, 2015; Southern *et al.*, 2015;

Fallgatter *et al.*, 2016) and shallow marine (Wright, 1977; Zavala *et al.*, 2006; Caineng *et al.*, 2012; Girard *et al.*, 2012; Silveira *et al.*, 2016) strata. A genetic relationship between hyperpycnal flows and turbidity currents within delta settings have also been reported elsewhere (*e.g.* Mulder *et al.*, 2003; Mutti *et al.*, 2003, Zavala *et al.*, 2006, Girard *et al.*, 2012), but the link between hyperpycnites and debrites are still poorly understood.

The main hypothesis of this research is that cohesive and non-cohesive deposits of study area are genetically related and triggered by hyperpycnal currents. This research aims to present the spatial distribution and the genetic link (physical connection) between cohesive and non-cohesive strata. This understanding will improve the knowledge about the distribution of reservoir properties on turbidite reservoirs associated with hybrid beds and debrites.

2. GEOLOGICAL SETTING

The Camaquã Basin is located in the central portion of the Rio Grande do Sul State, southernmost Brazil (Fig. 1). It rests on Neoproterozoic igneous and metamorphic rocks of the Sul-Riograndense Shield. The basin presents a NE-SW oriented, elongated shape. It is bounded by the Dom Feliciano and Tijucas belts (eastern margin) and São Gabriel Terrain and Rio de La Plata Craton (western border).

Most authors (Almeida, 1969; Almeida *et al.*, 1976, 1981; Wernik, 1978; Fragozo Cesar *et al.*, 1984; 2000; Chemale Jr. *et al.*, 1995; Paim *et al.*, 2000; Chemale Jr, 2000; Hartmann *et al.*, 2008) relate the Camaquã Basin to the late to post-collisional stages of the Brasiliano Orogeny.

According to Paim *et al.* (2000), the Camaquã Basin represents an Ediacaran to the Cambrian depositional *locus* of distinct basins. It records four tectonic-volcanic-sedimentary episodes evolving from compressive trough transpressive and distensive tectonic regimes (Paim *et al.*, 2014). This progression is represented by the Maricá retroarc foreland basin, East and West Bom Jardim strike-slip basins, East and West Santa Bárbara rifts and, at last, by the Guaritas Rift (Fig. 2).

The sedimentary record of the Santa Bárbara West Rift comprises coarse-grained intervals (mostly sandstones and minor conglomerates) intercalated with fine-grained sandstones and mudstones. Lenticular sandstones and conglomerates show small to middle-scale trough cross-stratification and frontal accretion surfaces and represent transverse bars on low sinuosity streams related to both braided and delta plains. Thin-

Bedded Turbidites (TBT), debrites, mudstones and sigmoidal sandstones encompass the main subaqueous delta and lacustrine facies (Paim *et al.*, 2014).

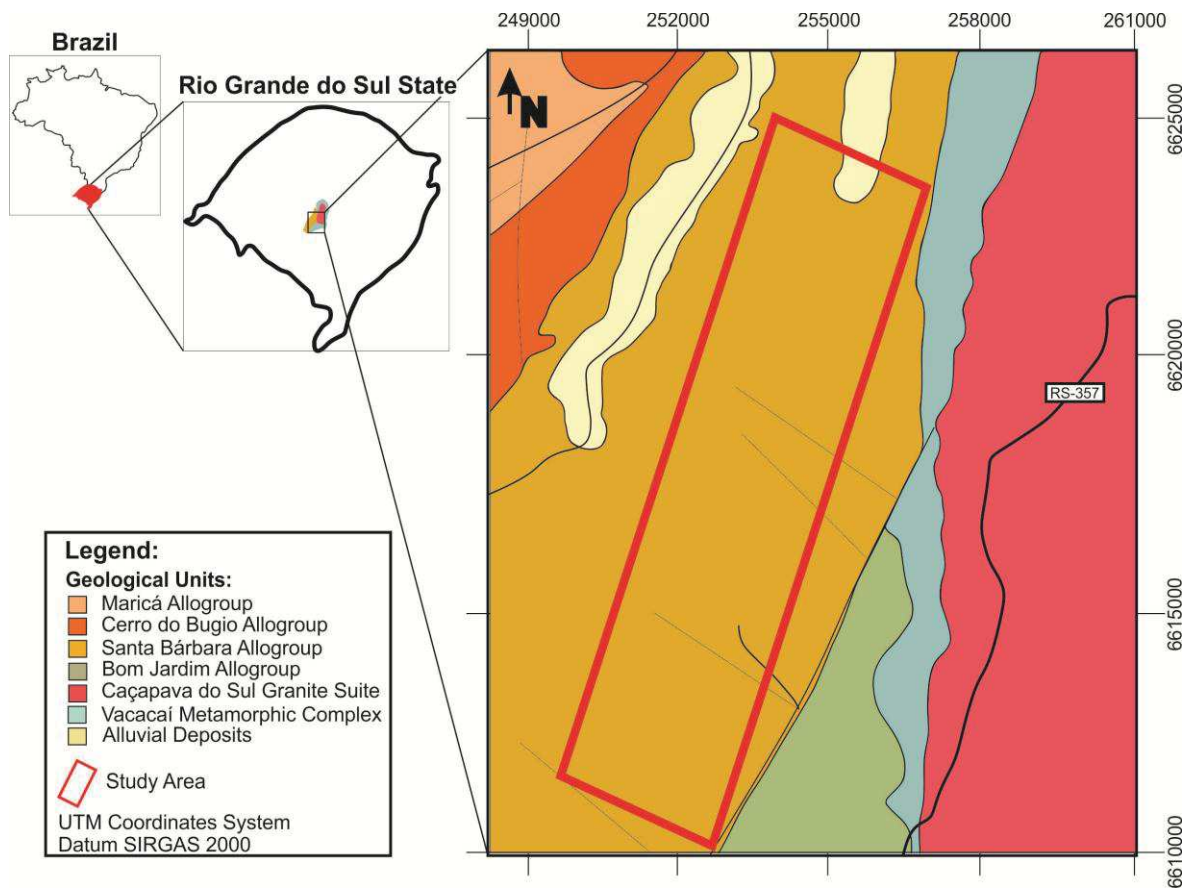


Figure 1 – Geological map indicating the study area (red rectangle). The Cerro do Bugio and Santa Bárbara allogroups dip about 20° to ESE, except close the fault along the southeastern margin of the Western Santa Bárbara Rift (modified from CPRM, 1995).

The Cerro do Bugio Allogroup includes acidic alkaline lavas and pyroclastic rocks at its base (Acampamento Velho Alloformation) and disconformably underlies the Santa Bárbara Allogroup (Borba & Mizusaki, 2003). Ages from detrital zircon grains of acid tuffs yielded the following maximum depositional ages for the base of Santa Bárbara Sub-basin: 573± 18 Ma (Chemale, 2000), 574± 7 Ma and 572± 6.5 Ma (Jenikian *et al.*, 2012). The Caçapava Granitic Complex represents the deformational event that generates the unconformity between Santa Bárbara e Guaritas allogroups. A leucogranitic sample of Caçapava Complex determined the minimal age of 541± 11 Ma for the top of Santa Bárbara strata. Zircons from outcrops at Ramada Plateau location bring the age of 553± 5.4 Ma for andesitic basalts and 549± 5 Ma for rhyolitic spills (Sommer *et al.*, 2005). Additional age control is also shown in Fig. 2. Therefore, an age ranging from 574 and 549 Ma is assumed for the Santa Bárbara Allogroup (Paim *et al.*, 2014).

The studied area includes the Upper Proterozoic metamorphic (Vacacaí Metamorphic Complex) and intrusive rocks of Caçapava do Sul Granite Intrusive Suite, older units of the Camaquã Basin (Maricá, Bom Jardim and Cerro do Bugio allogroups) and the entire Santa Barbara Allogroup. The studied interval is part of the Santa Bárbara Allogroup and corresponds to the upper part of the Serra dos Lanceiros Alloformation (Paim et al., 2000) and to the middle portions of the Santa Bárbara 1 Sequence (Almeida, 2001) (Fig. 3).

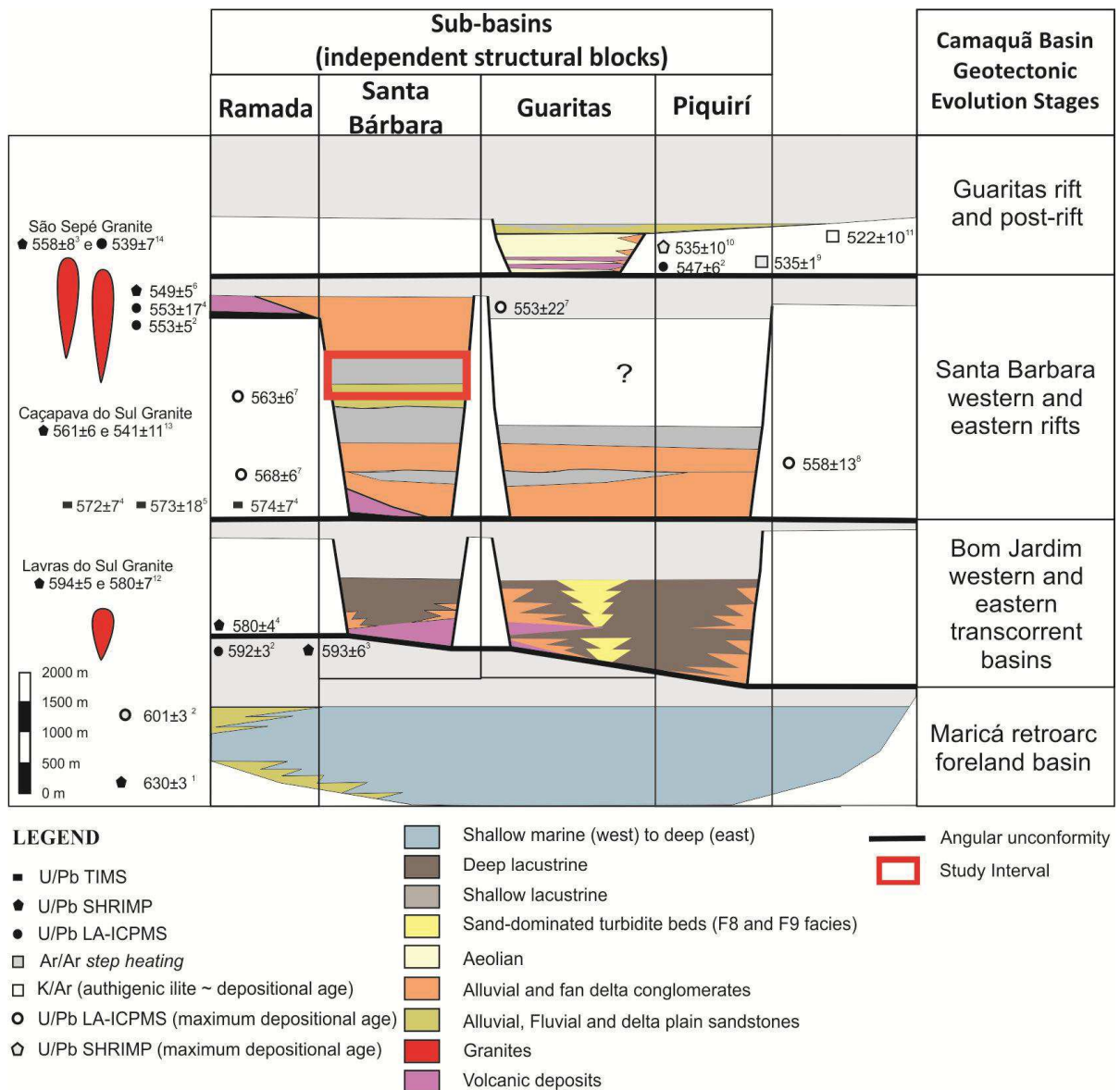


Figure 2 – Tectono-sedimentary evolution of the Camaquã Basin (modified from Silveira, 2016, after Paim et al., 2014).

3. METHODS

A photostratigraphic analysis of the study area was performed using aerial photographs (1:25,000) and satellite images (Google Earth). This approach was adopted due to the fact that the study succession is dipping about 20° to ESE. This methodology allowed the recognition of several stratigraphic key surfaces (sequence boundaries, transgressive and maximum flooding surfaces) as well as the main lithologies exposed along the study area.

The lithological associations were mapped on aerial image based on differences of relief, texture, color, and bed thickness and geometry. Sequence boundaries were defined by erosional truncation and the abrupt superposition of fluvial facies above subaqueous deposits. On the other hand, transgressive surfaces were defined by the abrupt superposition of subaqueous facies above fluvial deposits. The maximum flooding surfaces were delineated by the abrupt change on ground morphology, which indicates a change from fining- to coarsening-upward trends. Therefore, the facies associations were ascribed to three systems tracts (lowstand, transgressive and highstand) based on their relative position to the stratigraphic key surfaces and the internal stacking trends.

Based on the interpreted stratigraphic framework, one depositional sequence was chosen for a higher-resolution analysis due to its more complete nature and larger extent. Nine sedimentary logs (logs 1-9) were acquired in the selected interval to characterize vertical and lateral facies changes. Each sedimentological log is paired with a gamma-ray profile obtained from CPS (counts per second) readings at intervals of 10 cm. Facies description took into account usual features such as bed geometry, lithology, fabric and sedimentary structures. The discriminated facies were grouped into facies associations based on their longitudinal and vertical relationships.

Gamma-ray logs were used to show grain size changes and mud content. Usually, high and low gamma-ray readings in siliciclastic rocks suggest high and low mud content, respectively. However, the signature is higher and lower than expected readings for sandstone and mudstones, respectively. The values between 140-200 cps for sandstones can be explained by the presence of radioactive elements such as K-feldspar and clay minerals. Based on the comparison between readings and actual lithologies, a value of 200 cps was adopted to differentiate mud-rich from sand-dominated lithologies.

Optical microscopy was used to identify the presence, grain size and type of the fine-grained matrix. X-ray diffraction and SEM (Scanning Electron Microscope) analyses

were made to identify the mineralogy of the matrix, in special clay minerals. These analyses were performed to help in the differentiation of mud-rich (cohesive) from mud-poor (non-cohesive) deposits from proximal to distal reaches of the studied depositional system.

4. RESULTS

4.1 FACIES AND FACIES ASSOCIATIONS

Eight sedimentary facies were identified based on grain size, fabric and sedimentary structures. They will be individually described and interpreted (see also Table 1) and then grouped into three facies associations related to specific environments and/or sub-environments.

4.2 Facies analyses

4.2.1 Massive sandstone – Sm

Description: It comprises massive and structureless, 3 to 30 cm thick tabular beds composed of fine- to medium-grained sandstone (Fig. 4). Some beds shows coarse grains concentrated at the base. Flame structures and pipes along the base and top of the beds, respectively, are also present.

Interpretation: Its lateral continuity and widespread occurrence indicate non-confined flows. The massive nature of the facies suggests frictional freezing rather than layer-by-layer deposition as the main depositional mechanism. Fluid escape features point to high-concentration flows during the depositional stage. On the other hand, coarse grains concentrated at the base of some beds indicate fluid turbulence as a major support mechanism during earlier stages of the flow. Such characteristic indicates high-concentration turbidity current (Walker, 1978) or concentrated density flow (Mulder & Alexander, 2001), and may be ascribed to the basal, granular layer of bipartite flows (Sanders, 1965) or Ta interval of Bouma (1962).

4.2.2 Trough-cross bedded sandstone - St

Description: Beds are lenticular to sigmoidal and 10 to 50 cm thick. They are composed of fine- to medium-grained sandstone with small- to medium-scale trough-cross bedding (Fig. 4). Coarse-to very coarse-grained sand particles, granules and few cm wide mudstone clasts are commonly present and highlight cross-stratification planes. Cross-

bedding occurs either as single or superimposed sets, associated with gentle slopes that dip down-stream. This facies is replaced down current by ripple-cross-laminated sandstones, which fills up small depressions. Cross-bedding readings indicate dominant paleocurrent to NE.

Interpretation: Isolated or superimposed, sigmoidal sets of St that thin out downstream point to frontal accreting-bedforms (isolated sets) or bars (compound sets) deposited by bedload right at the distributary mouths on a proximal delta front. Their downcurrent replacement by ripple cross-laminated sandstone indicate that effluents also include a finer-grained, suspended-load that was transported further downstream along a gentle slope and deposited by traction plus sand fallout. Paleocurrent readings indicate a consistent NE transport along the inner portions of the delta front.

4.2.3 Undulated Sandstone - Su

Description: Sandstone beds are 10 to 50 cm thick and limited by undulating to irregular bounding surfaces with both concavities and convexities preserved. Cross bedding ranges from tangential (high-angle) to parallel (low-angle) to bedding planes (Fig. 4). This facies is composed of fine- to medium-grained sandstone. Coarse sand grains, granules and mud clasts dispersed along the stratification occur only in the mid portion of the system. Although usually amalgamated, sandstone beds might be separated by 0.5-1 cm thick mudstones.

Interpretation: The above described features suggest the co-existence of both dunes and rounded, low angle bedforms. Whereas the first ones unequivocally represent flow regime subaqueous dune related to unidirectional current, the second one could be ascribed to storm- (Dott & Bourgeois, 1982; Harms *et al.*, 1982; Walker *et al.*, 1983), combined (Wheatcroft, 2000) oscillatory flows; hyperpycnal flows (Wright *et al.*, 1988; Mutti, 1992; Mutti *et al.*, 1996, 2003) or simply to unidirectional flows under transitional flow regime conditions (Fielding, 2006; Allen *et al.*, 2014). General paleocurrent data indicate unidirectional flow. Also, there is a generalized lack of classical features related to oscillatory flows, such as wave ripples. Therefore, deposition of this facies is here related to transition between lower and upper flow regime on proximal delta front settings. It is comparable to the flood-generated delta front sandstone lobes of Mutti *et al.* (2000).

4.2.4 Graded Sandstone to mudstone couplets - Sg

Description: It is characterized by 5 to 20 centimeter thick, tabular beds of normal graded, fine- to very fine-grained sandstone. A 1 to 5 cm thick mud cap is occasionally present. Sandstones include, from base to top, plane-bedding with parting lineation and climbing ripple-cross lamination (Fig. 4), that present paleocurrent trend to NE. This facies includes mud clast-rich layers at the intermediate portions of the area.

Interpretation: Its tabular geometry indicates widespread flows. Normal graded sandstone beds associated with upward change from horizontal to ripple-cross lamination suggest waning currents, low concentration turbulent flows. Therefore, this facies was assigned to short-lived (surge-type) low concentration turbidity currents. It is equivalent to the surge-type turbidites of Mulder & Alexander (2001). The mudstone cap represents the deposition of the remaining plume.

The absence of mud clasts in proximal area and the increase of mud clast and mud content along the intermediate and distal reaches could be related to erosion of non-lithified mud along the subaqueous realm. Mud clasts show evidences of fragmentation and disaggregation, which could explain the gradual downstream clay-enrichment of the matrix.

4.2.5 Inverse to Normal Graded Sandstone - Sin

Description: Beds are 5 to 10 cm thick and composed of fine- to very-coarse-grained sandstone. They include inverse to normal grading, internal scours and alternation of plane-bed and ripple-cross stratification (Fig. 4).

Interpretation: All together, inverse and normal grading, internal scours and alternating upper and low flow regime structures within a single bed indicate accelerating and decelerating stages of a long lived current. In addition, it is possible to delineate a physical connection of these deposits to the proximal delta front and delta plain fluvial facies. Therefore, these features suggest hyperpycnal flows (Bates, 1953) related to quasi-steady hyperpycnal turbidity currents (Mulder & Alexander, 2001).

4.2.6 Clayey sandstones - SC

Description: It comprises a mixture of fine- to very fine-grained sandstone and -mudstone with much larger clasts (coarse- to very-coarse sand grains, granules and rarer pebbles) dispersed within a clay-rich matrix. Beds are 2-10 cm thick, tabular and massive (Fig. 4).

Interpretation: Its tabular geometry and the lateral continuity indicate widespread flows. The massive nature associated with outsized clast floating in the matrix, indicate *en masse* freezing of cohesive flows (Lowe, 1982). Its clay content indicates matrix strength as the main grain support mechanism on the flow (debris-flow).

4.2.7 Silty sandstone - SS

Description: It is a mixture of fine- to very fine-grained sandstone with coarse- to very-coarse sand grains, granules and rarer pebbles floating in a silty matrix (Fig. 4). Beds are 3-10 cm thick, tabular and massive.

Interpretation: The massive nature associated with the presence of floating, outsized clasts and lack of clay indicate frictional freezing of non-cohesive, highly concentrated flows. This sort of flow has been called hyperconcentrated density flows (Mulder & Alexander, 2001), sandy debris flows (Shanmugam, 1996), non-cohesive or cohesionless debris flows (Nemec & Steel, 1984), catastrophic flood deposits (Mutti *et al.*, 1996), inertial grain flows (Takahashi, 1981) and grain-flow avalanches (Leeder, 1999), and also related to specific portions (transitional layer) of slurry flows (Lowe & Guy, 2000). From the proposed names, sandy debris flows seems more appropriated to the case due to the sandy nature of the facies. Suspended grains within sandy debris flows are supported by matrix strength, frictional strength, and buoyancy (Shanmugam, 1996). Deposition takes place by frictional freezing resulting from grain-to-grain interaction (Mulder & Alexander, 2001).

4.2.8 Mudstone - F

Description: Tabular, 10-35 cm thick, massive, muscovite-rich beds composed of fine- to medium-grained silt and subordinate clay. Mud cracks commonly occur at the base of these fine-grained packages (Fig. 4). However, although rarer, mud cracks also occur at the mid portions of these muddy intervals.

Interpretation: The massive nature and tabular geometry indicate deposition of silt and clay from fine-grained plumes on usually low energy settings. The presence of mud cracks indicates subaerial exposure as a result of high-frequency regressive pulses. However, its occasional presence in the mid of the mudstone intervals indicates eventual base-level falls due to drier conditions. The mica-rich nature of the mudstone could be explained because these grains settle down as fine-grained particle in the flow due to their platy shape.

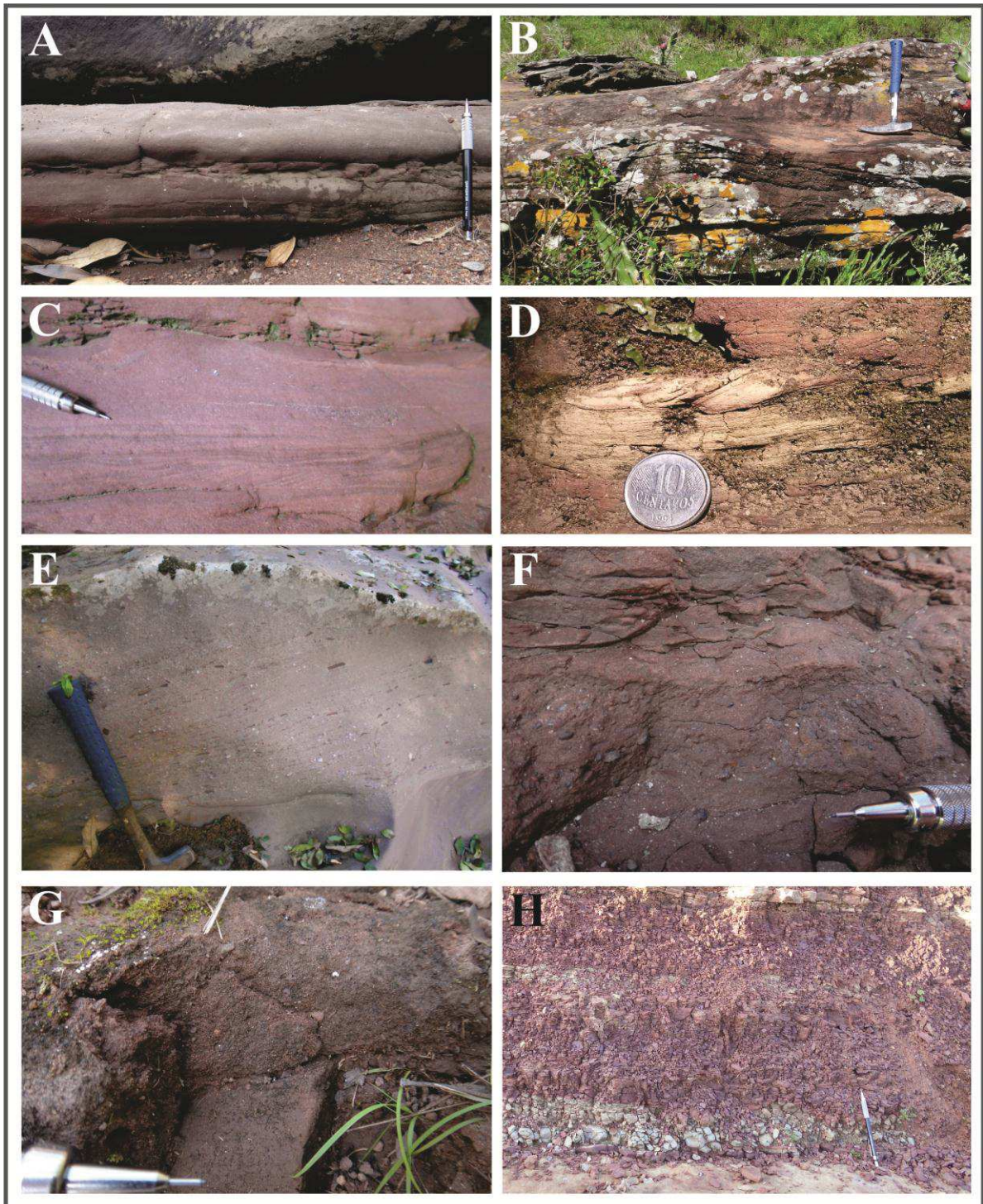


Figure 4 – Facies table. A) Massive sandstone with flame structure at the base; B) Amalgamated and truncated Su beds; C) Sin bed with alternation of lower and upper flow regime sedimentary structures and internal scours; D) Graded sandstone beds displaying upper flow regime plane bedding near the base and climbing ripple-cross lamination in the upper part of the beds; E) Trough-cross bedded sandstone bed with granules and mud clasts; F) Detail of a thin SC bed with dispersed coarse sand grains and granules; G) 3 cm thick SS bed; H) Mudstone-rich interval.

Table 1 – Description and interpretation of the sedimentary facies discriminated in the study area:

Facies	Grain Size	Fabric	Position	Geometry and structures	Interpretation
Sm – Massive Sandstone	Fine- to medium-grained sandstone	Massive	Proximal and intermediate	Tabular geometry. Flame structures on the base and pipes in the upper parts of the beds	Unconfined, high concentration turbidity currents
St – Trough-cross Bedded Sandstone	Fine- to medium-grained sandstone	No or normal grading	Proximal	Lenticular to sigmoidal geometry. Cross-bedding either as single or superimposed sets associated with gentle, down-dip slopes	Distributary mouth bars deposited by unconfined unidirectional flow in proximal delta front
Su – Undulated Sandstone	Fine- to medium-grained sandstone	No grading	Proximal	Lenticular geometry. Tangential or undulating, high- to low-angle cross bedding. Both concavities and convexities are preserved	Transition between dune and upper flow regime plane bed stability fields on a proximal delta front
Sg – Graded Sandstone to Mudstone Couplets	Fine- to very fine-grained sandstone and mud	Normal grading	Intermediate and distal	Tabular beds. Upper flow regime plane bedding followed by climbing ripples cross lamination, eventually capped by mud	Unconfined, surge-type, low concentration turbidity currents
Sin – Inverse to Normal Graded Sandstone	Fine- to very coarse-grained sandstone	Inverse to normal grading	Intermediate and distal	Tabular geometry. Beds include internal scours and alternation of lower and upper flow regime bedding	Unconfined, accelerating and decelerating quasi-steady hyperpycnal turbidity current
SC - Clayey Sandstone	Fine- to very fine-grained sandstone and mudstone	Massive, chaotic	Distal	Tabular geometry. Matrix supported, clay-rich sandstone with dispersed coarse sand grains, granules and mud clasts	<i>En masse</i> deposition from a cohesive, unconfined debris flow
SS – Silty Sandstone	Fine- to very fine-grained sandstone and siltstone	Massive, chaotic	Distal	Tabular geometry. Matrix supported, silt-rich sandstone with dispersed coarse sand grains, granules and mud clasts	Frictional freezing of a non-confined sandy debris flow
F – Mudstone	Fine- to medium-grained silt and subordinate clay	Massive	Intermediate and distal	Tabular geometry. Mud cracks at the base of the muddy intervals	Mud fall out from suspension plumes

4.3 Microscopic Analyses

4.3.1 Petrography

Petrographic analysis was used to identify the presence and type of fine-grained matrix within the Sg, SC and SS facies, therefore to understand changes on flow rheology along the depositional tract. Besides, sandstone grains provide general clues about source area composition and distance.

Sandstone particles are sub-angular to sub-rounded, usually with low sphericity. They are composed of mono and polycrystalline quartz, K-feldspar, plagioclase, muscovite, volcanic and metamorphic fragments, mud clasts and rare heavy minerals (Figs. 5 and 6). Analyzed facies show inter and intra-granular hematite cement, sometimes as thin coatings around detrital grains. Silica occurs as quartz overgrowth precipitated after hematite cement, therefore indicating an eo-diagenetic origin for the later. These deposits also present inter- and intra-granular calcite cement precipitated after the previous cements either as poikilotopic pore-filling or replacing feldspar/ plagioclase grains.

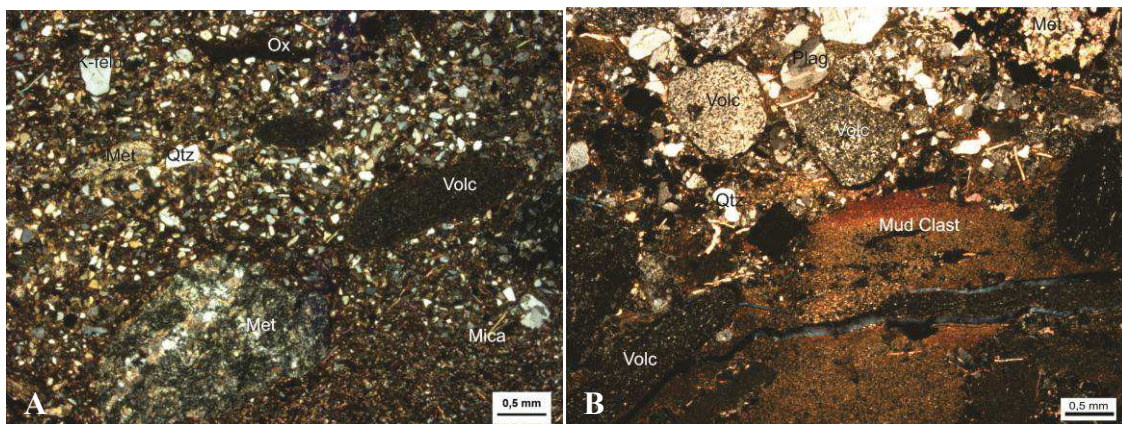


Figure 5 – Photomicrographs under polarized light illustrating composition and fabric of Sg facies. A) Sandstone composition; and B) partially fragmented mud clast and contorted, detrital mica grains. Volc=volcanic fragment, Plag=plagioclase, Met=metamorphic fragment, Q=quartz, K-feld=K-feldspar.

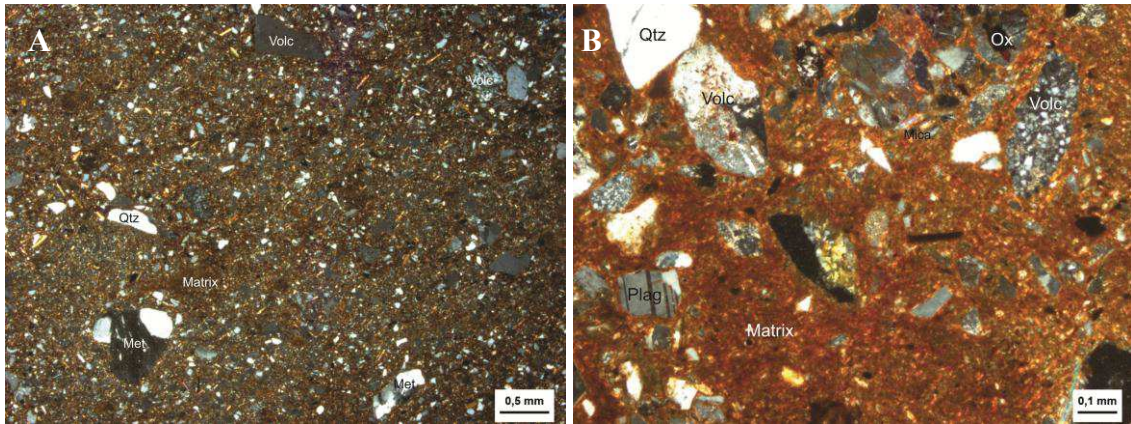


Figure 6 – Photomicrographs under polarized light showing sand grains (quartz, plagioclase and volcanic fragments) dispersed in a silty (A) and clayey (B) detrital matrix related to the SS and SC facies, respectively, Volc=volcanic fragment, Plag=plagioclase, Met=metamorphic fragment, Q=quartz, K-feld=K-feldspar.

The sub-angular and low sphericity indicates nearby sources whereas their composition point to different source areas. Gneisses, micas and polycrystalline grains of quartz suggest metamorphic sources; volcanic grains point to a nearby volcanic source and elongated mud clasts indicate intra basinal sources. Along the intermediate to distal reaches of the studied succession, the Sg, SC and SS facies include higher mud clast content relative to the proximal areas. Both macro and microscopic analyses show a progressive fragmentation of mud clasts and ensuing incorporation of mud into the matrix (Fig. 7).

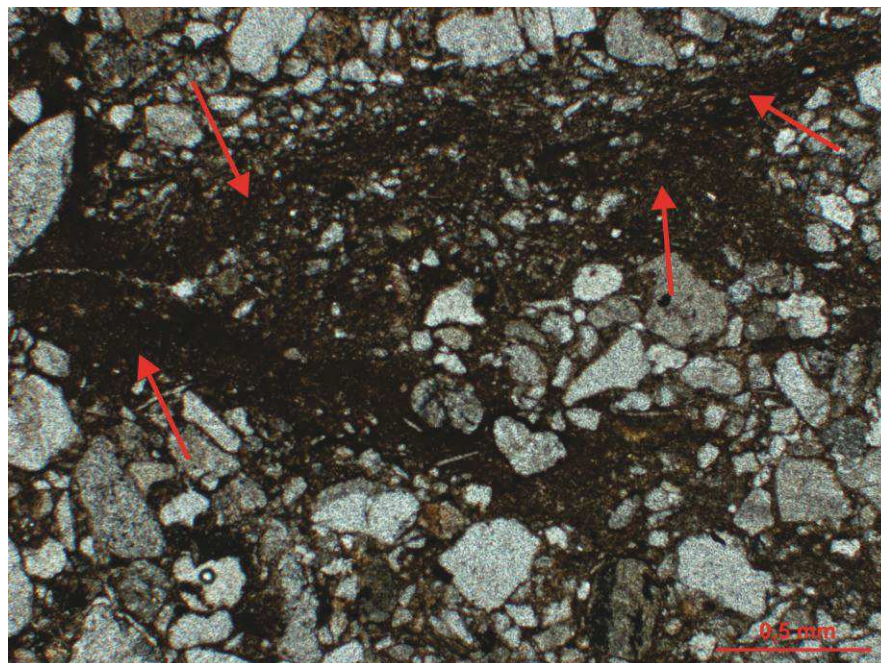


Figure 7 – Mud clasts fragmentation (indicated by narrow) and mud incorporation into the matrix.

Hematite cementation is related to eo-diagenesis, so to oxidizing conditions in the depositional setting. Hematite is usually derived from the breakdown of unstable iron-rich detrital minerals (*e.g.* augite, amphibole, olivine and biotite) and produces an intense red color in the framework and matrix (Ulmer-Scholle *et al.*, 2014). Hematite precipitation as grains coatings indicates long periods of exposure in a thick vadose zone typically found in sub-humid to arid climate (Walker, 1976).

The origin of silica cement is frequently associated with pressure dissolution of quartz grains, feldspar-alteration and clay-mineral transformations (Worden & Morad, 2000). Silica-rich solution migrates and precipitates as quartz overgrowths when super saturation is achieved (Tucker, 2001). Silica cementation took place after the precipitation of iron oxide as thin coats around some grains (Fig. 8). According Worden & Morad (2000), during shallow-burial small amounts of quartz overgrowths may precipitate in sufficient quantities to support the sandstone framework and inhibit compaction loss of intergranular porosity. This porosity can be further filled by other cements, as carbonates. This process seems to be reflected in the study rocks, with iron oxide and silica cements as eo-diagenetic cements followed by carbonate cementation.

Carbonate cement is composed of calcite and supposed to represent a mesodiagenetic process as it covers both hematite and silica cements and replace lithic and feldspar grains (Fig. 9). The arrangement of calcite around grains with sutured contact also indicated post-compaction, late cementation (mesodiagenesis). Mesodiagenetic carbonate cements may derive from the sandstones themselves, from juxtaposed successions as well as from groundwater migrating from deeper parts of the basins along fractures (Morad, 1998). Sources of Ca for the calcite cementation are many, but the dissolution of Ca-plagioclase is considered as an internal source of calcium (Shultz *et al.*, 1989).

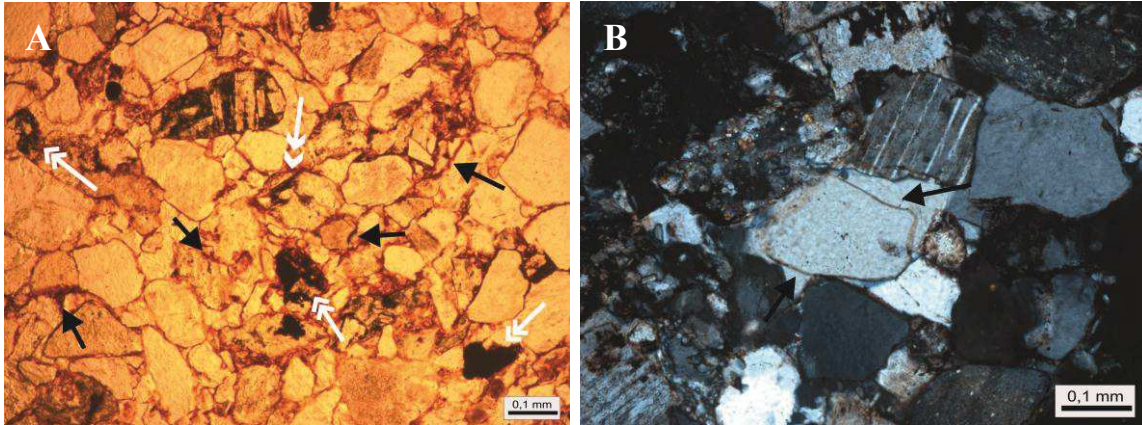


Figure 8 –Iron oxide cementation. A) Iron oxide coating (black arrows) and grains fillings (white double arrows); B) Quartz overgrowth (arrow). Note the original quartz shape delineated by thin iron oxide coating.

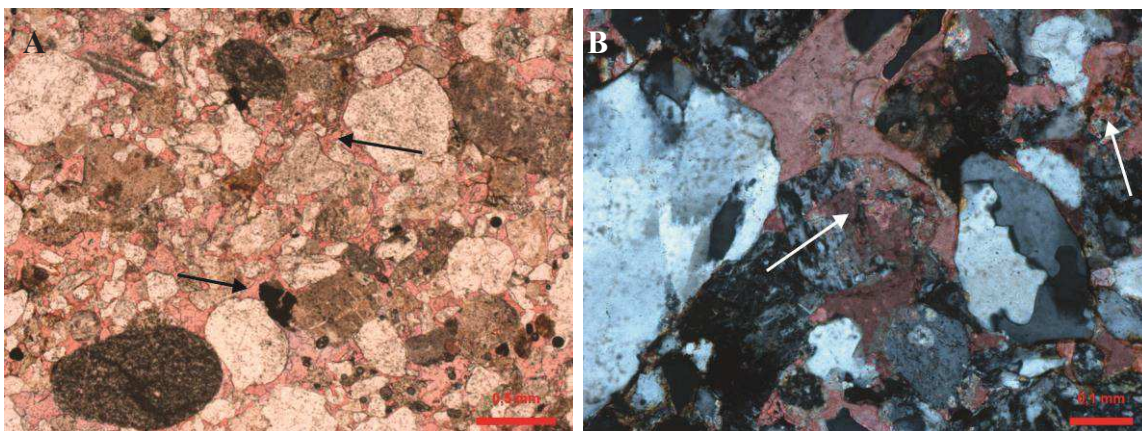


Figure 9 – Calcite cement highlighted by Alizarin Red. A) Calcite cement filling pores; B) High birefringence and relief calcite cement replacing lithic grains.

5.3.2 X-Ray and Scanning Electron Microscopy

X-ray diffraction (XRD) and Scanning Electron Microscopy (SEM) were used to analyze the composition of the clay minerals in the matrix of the SC facies. Samples were collected in both proximal and distal settings in order to verify any possible downslope change on detrital matrix composition.

X-ray results and petrographic analysis indicate that the detrital constituents of the matrix of all samples are quartz, as the main component, followed by muscovite, albite, microcline and vermiculite (Fig. 10). Hematite, silica and calcite are the cements. Therefore, composition of this facies is similar from proximal to distal reaches and includes vermiculite as the clay mineral present in the matrix.

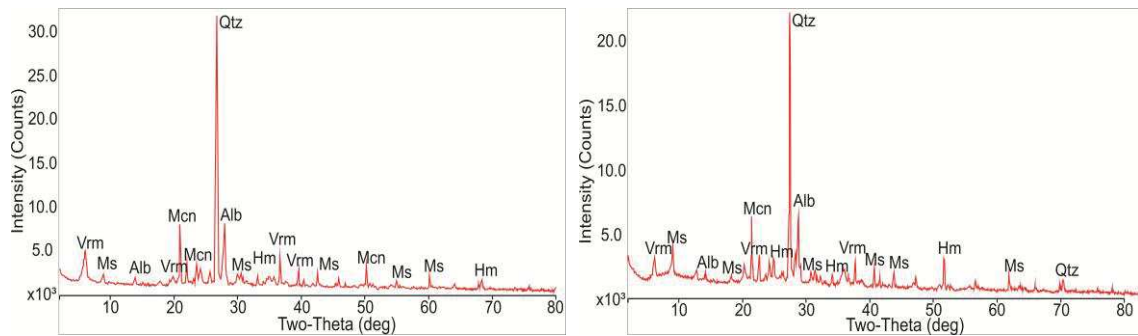


Figure 10 – X-ray diffraction graphics of proximal (left) and distal (right) debrites samples (SC facies). Notice that they present similar composition and include vermiculite in the matrix.

SEM analyses of proximal and distal samples were also performed. EDS diagram of the matrix show a chemical composition that matches the mineralogical results found in the XRD and petrography. Therefore, Si is the most abundant element followed by Al, K, Mg Na, Fe, Ti and Ni. It is worth to notice the occurrence of Mg in the chemical composition, which re-enforces the interpretation of the XRD diagrams and SEM images that indicated the presence of vermiculite (Figs. 11 and 12).

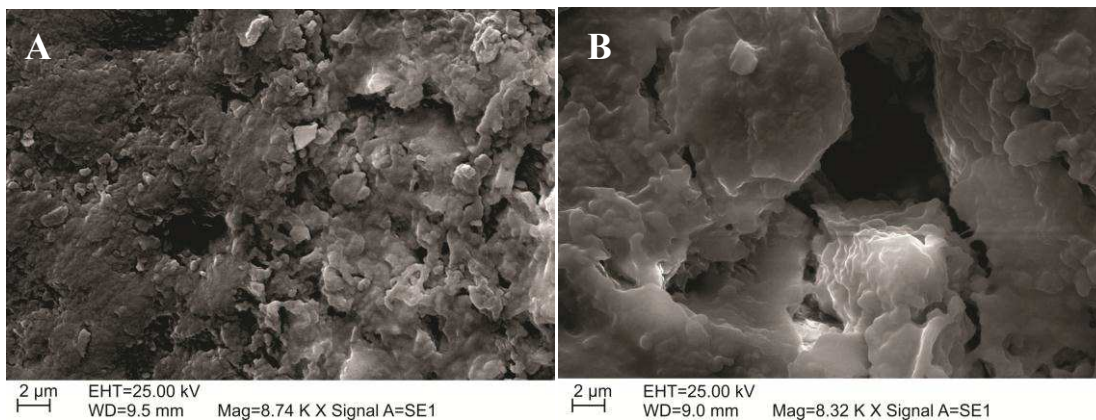


Figure 11– SEM images of clay minerals. A) Contact between mud clast (left) and the clay mineral in the matrix (right); B) Zoom of the right zone of A) showing vermiculite crystals covered by microcrystalline, botryoidal quartz.

Element	Weight %	Atomic %
Na	0.72	0.92
Mg	1.57	1.90
Al	4.45	4.84
Si	82.45	86.04
K	2.44	1.83
Ca	0.74	0.54
Fe	5.36	2.81
Ni	2.25	1.13
Totals	100.00	

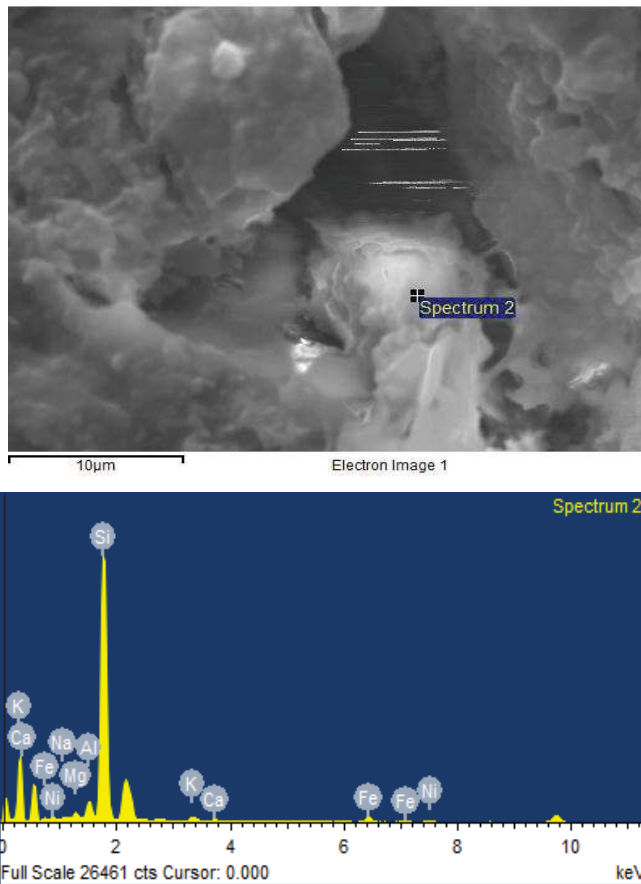


Figure 12 – SEM image and EDS graphic representation and related compositional table.

4.4 Facies Associations

4.4.1 Facies Association 1

The proximal, SSW portion of study area is mostly characterized by Undulated (Su), Trough-Cross Bedded (St) and Massive (Sm) sandstone facies, which are well-represented in Log C.

This facies association encompasses transitional flow regime bedforms (Su) and mouth-bar avalanche foresets (St) as well as high-concentration turbidites (Sm). The lack of channel forms, the laterally-extensive bed geometry, the unidirectional nature of the flows, the down-current transition to tabular turbidites (facies association 2) and mouth-bar setting ascribed to the St facies suggest a proximal delta front facies association deposited along a gentle slope (Fig. 13).

4.4.2 Facies Association 2

The mid portion of the study area is also sand-prone and well-recorded in logs D and G (Fig. 14). It is represented by abundant Graded Sandstone to Mudstone Couplets (Sg), Massive (Sm) and Inverse to Normal Graded (Sin) sandstones, less common Undulated (Su) and Trough-Cross Bedded (St) sandstones and scarce Clayey (SC) and Silty (SS) sandstones.

The depositional setting was dominated by turbidity currents. The dominant low-concentration turbidity currents were ascribed to both short-lived (Sg) and quasi-steady hyperpycnal (Sin) turbidity flows whereas high-concentration, surge-type turbidity flows are rarer (Sm facies). Mudstones (F) were ascribed to the settling of fine-grained grains from hypopycnal plumes during low energy phases. On the other hand, the scarcer SC and SS facies represent the occasional event of cohesive (debrites) and non-cohesive (sandy debrites) flows, respectively. The presence of Su and St facies indicates eventual influence of proximal delta front processes.

Therefore, this facies association represents a subaqueous environment dominated by turbidity currents, but eventual cohesive to non-cohesive debris flows may also play a role. In total, the sand-prone nature, the presence of proximal delta-front deposits and downdip transition to finer-grained facies point to an intermediate portion of the delta front (Fig. 13).

4.4.3 Facies Association 3

The northern portion of the study area comprises interbedded sandstones and mudstones that are well recorded in logs B, E and H (Fig. 13). Graded Sandstone to Mudstone Couplets (Sg), Inverse to Graded Sandstone (Sin), Mudstone (F), Massive Sandstone (Sm), Clayey Sandstone (SC) and Silty Sandstone (SS) correspond to the main facies of this association. The Sg, Sin and Sm sandy facies register low-concentration turbidites, hyperpycnal turbidites and high-concentration turbidites, respectively. On the other hand, SC and SS facies are related to cohesive and cohesionless debris flows, respectively. St facies is very rare, indicating uncommon influence of proximal delta front processes in this portion of the system.

Based on facies proportions, this depositional setting was dominated by turbidity currents, although debris flows and mud fallout become more frequent. The turbidity

currents are related to both short-lived (Sg) and quasi-steady hyperpycnal (Sin) currents. On the other hand, the proportion of cohesive (SC) and non-cohesive (SS) debris flow deposits increases relative to the previous facies associations. This increase indicates that a change from fluidal to cohesive rheology of the gravity flows were favored along a downstream direction, possible due the progressive mud incorporation from substrate. Besides, a vertical association between turbidites and debrites was also identified. Several beds comprise a debrite interval superimposed by very fine-grained sandstone, eventually including a mudstone cap. These beds represent hybrid flows.

The sand-to-mud ratio also increases relative to the previous facies associations, as expressed by the more common presence of Mudstones (F). This increase on mud content suggests more distal settings favoring the deposition and preservation of fine-grained grains derived from hypopycnal plumes. These evidences suggest a distal delta front close to a prodelta-lacustrine setting where turbidity, debris and hybrid flows acted together with mud fall-out (Fig. 13).

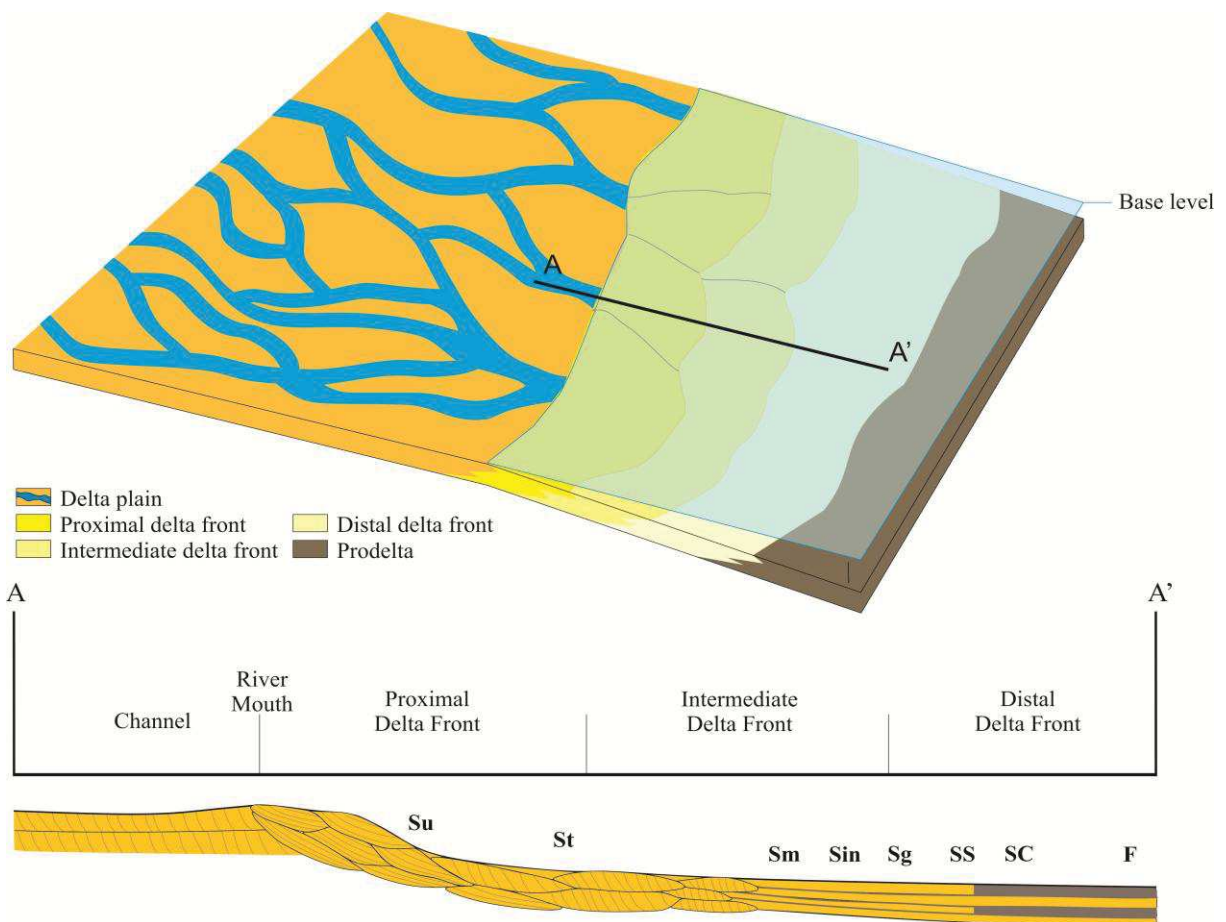


Figure 13 – Conceptual depositional model and facies tract, including proximal, intermediate and distal reaches of a delta front (facies association 1, 2 and 3, respectively). The A-A' section shows the facies distribution along the delta front.

4.5 Facies Tracts

Facies tracts represent the downcurrent changes on facies and are supposed to represent changes on transport and depositional mechanisms. This approach is here used to evaluate the genetic relationships between turbidites and debrites. As previously stated, exposures are not abundant or extensive, and are scattered within distinct systems tracts. To avoid any conclusion that could be related to different accommodation rates rather than changes on sedimentological processes, the proximal to distal facies changes will firstly be analyzed along each systems tract. If no difference is found, it seems then plausible to exclude accommodation as a major control on flow transformation.

4.5.1 Sequence Stratigraphy

Based on photointerpretation, it was possible to delineate two other unconformities (sequence boundaries) within the Serra dos Lanceiros Alloformation. Therefore, instead of a single depositional sequence, as formerly assumed, this unit comprises three depositional sequences (Figs. 14). Each sequence record a basal, lowstand system tract (fluvial and/or delta deposits) followed by a transgressive surface, and succeeding transgressive systems tract (upward deepening delta facies succession). The TST ends at a maximum flooding surface that is finally overlain by the highstand systems tract (upward shallowing delta facies succession). Due to its extent and better exposures, the subaqueous delta facies of the intermediate depositional sequence were described for the sedimentological study.

ascribed to the Lowstand System Tract - LST (Fig. 13). The downdip facies change along this systems tract is exemplified by three sedimentary logs (C, D and E - Figs. 14 and 15).

Gamma ray readings show a clear downdip decrease on the sand-to-mud ratio (Fig. 15). This ratio ranges from about 1 at the proximal (Log C) through 0.7 at the intermediate (Log D) to 0.3 at the distal (Log E) reaches.

High-concentration turbidity currents are well represented in the proximal settings (Log C) and almost disappear at the intermediate portions (Log D). On the other hand, low concentration turbidites are scarce in the proximal settings, but become abundant in the intermediate portions. Therefore, it seems logical to suppose that the disappearance of the high-concentration turbidites and the appearance of the low-concentrated ones are not casual, but a result of downdip flow transformation.

Low-concentration turbidites are abundant in the intermediate settings and decrease towards the distal portions of the system (Log E). On the other hand, debrites are absent in the proximal areas and rare in the intermediate settings, but become more common towards the distal portions. Therefore, it seems also logical to state that the decrease of the low-concentration turbidites and the appearance of debrites are not casual, but a result of a subsequent downdip flow transformation. The change from a turbulent turbidity current to debris-flows is also coincident with the down-dip increase on the amount of mud-rich facies, from where mud particles could be incorporated into formerly turbulent flow.

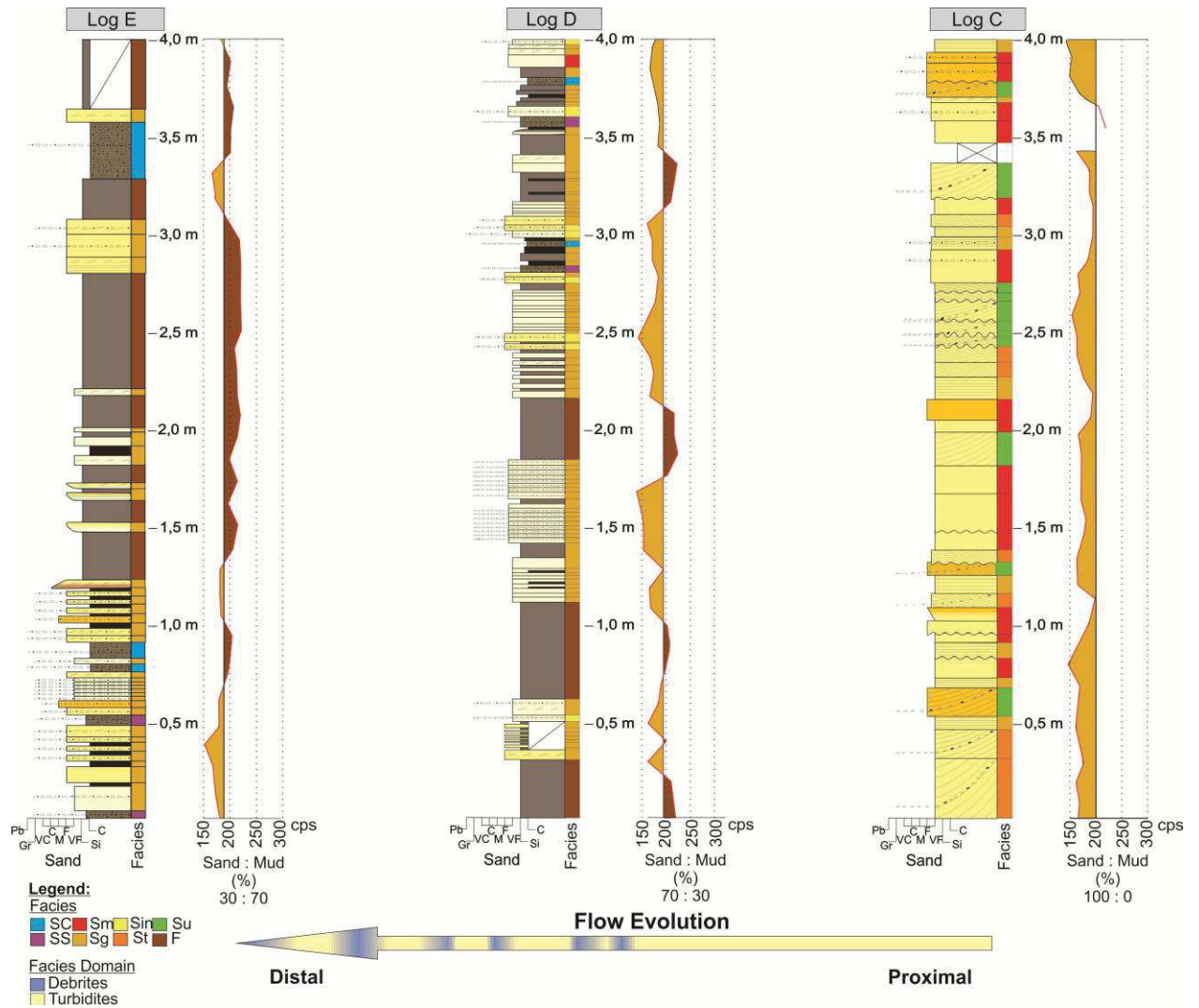


Figure 15 – Facies tracts demonstrated in three sedimentary logs described on delta front strata of the lowstand system tract. The logs are disposed from proximal (Log C), through intermediate (Log D) to distal (Log E) areas.

4.5.1.2 Transgressive Systems Tract (TST)

The retrogradational, intermediate portion of the mid depositional sequence corresponds to a transgressive system tract (TST). It is bounded by the transgressive (below) and maximum flooding (above) surfaces and shows a downdip change from facies association 1 to 2 and 3. Two sedimentary logs (Figs. 14) described near the maximum flooding surface (logs A and B) are used to show the downdip facies changes (or facies tract).

Like the previous system tract, the transgressive one also shows a downdip decrease on the sand-to-mud ratio well: about 0.9 in the proximal (Log A) and near 0.55 in the distal (Log B) areas (Fig. 16).

Again, high-concentration turbidites are represented in the proximal reaches (Log A), but disappear at intermediate settings (Log D). On the other hand, low concentration turbidites are absent in the proximal setting and become abundant in the intermediate portions. Therefore, the disappearance of the high-concentration turbidites and the appearance of the low-concentrated ones seem again be the result of a downdip flow transformation. Like the low-concentration turbidites, the debrites are also absent in the proximal area, but become abundant in the mid reaches. Therefore, it seems logical to suppose some sort of connection between the presence the low-concentration turbidites and debrites. The development of turbulent turbidity currents and debris-flows could again reflect the erosional nature of the first ones.

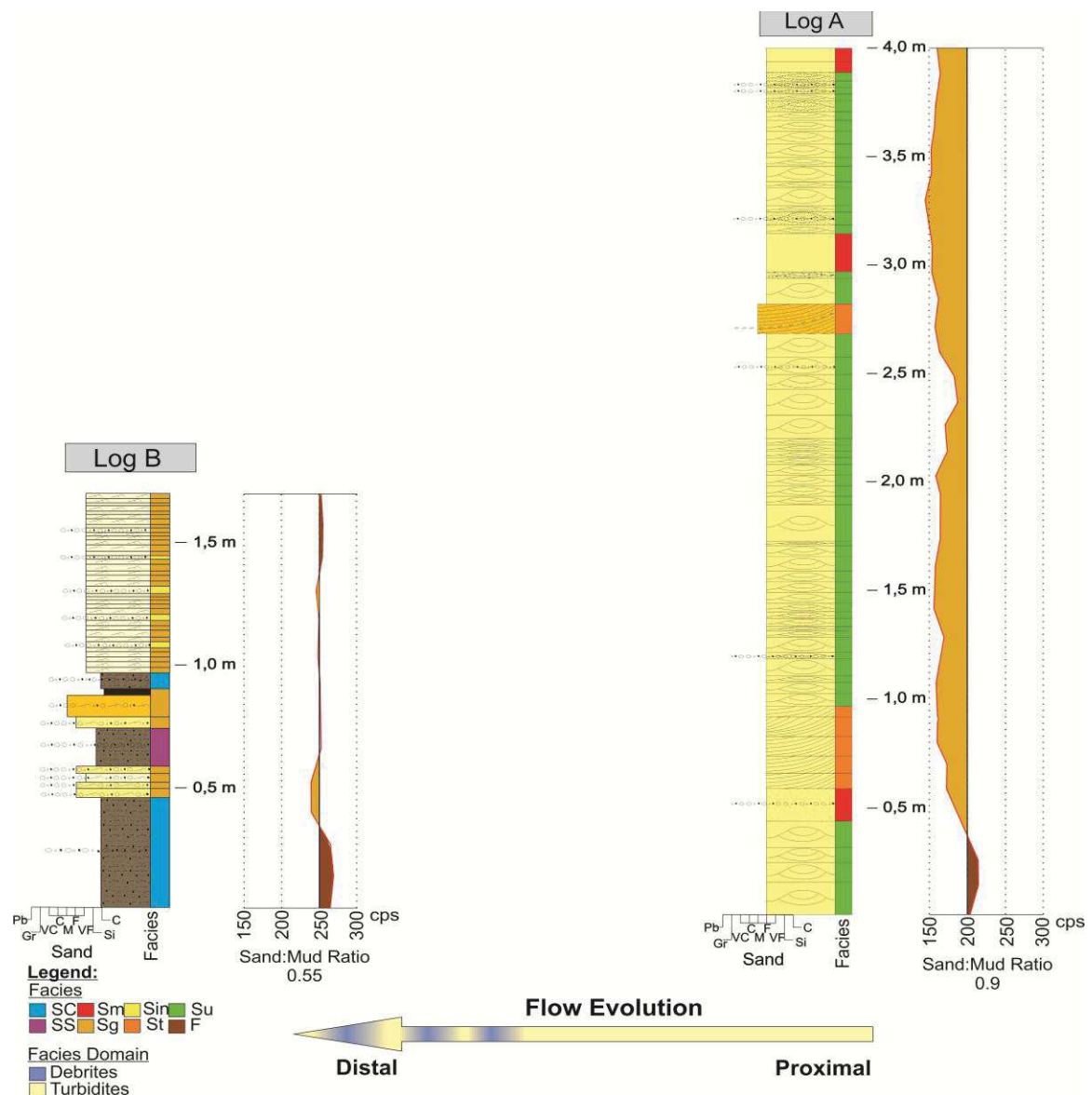


Figure 16 – Facies tracts demonstrated in sedimentary logs related to the transgressive system tract. Both logs acquired near the MFS. Log A represents proximal settings and Log B distal ones. The proportion of sand and mud is expressed on gamma ray graphics.

4.5.1.3 Highstand System Tract (HST)

The upper portion of the mid depositional sequence shows an aggradational to slightly progradational stacking trend as well as a downdip change from facies association 1 through 2 to 3. A maximum flooding surface and an unconformity delineate the lower and upper boundary of this HST (Fig. 14). The downdip facies change along this systems tract is exemplified by three sedimentary logs (F, G and H - Figs. 14 and 17).

A downdip decrease on the sand-to -mud ratio is again clearly recorded in the gamma-ray logs (Fig. 17). Sand-to-mud ratio ranges from 0.95 in the proximal (Log F) through 0.8 in the intermediate (Log D) to 0.5 in the distal (Log H) reaches.

Turbidites are dominant in the proximal settings (Log F). However, whereas the relative amount of high-concentration turbidites fast decreases towards the intermediate portions of the system, (Log G), the contrary happens with the low-concentration turbidites. This downdip change on the relative proportion of both types suggests that high-concentration currents are replaced by low-concentration flows as a result of a downdip flow transformation.

As above mentioned, low-concentration turbidites are abundant in the mid-portions of the system, but they decrease downdip (Log H). On the other hand, the debrites, which are absent in the intermediate and proximal areas, become more common towards the distal portions. Therefore, the decrease of the low-concentration turbidites and the appearance of debrites are interpreted again as the result of a subsequent downdip flow transformation. Once more, the change from turbulent underflows to debris-flows coincides with a downdip increase on the amount of mud-rich facies. A mechanism of mud clasts incorporation into the turbulent flow is again advocated to explain this flow transformation.

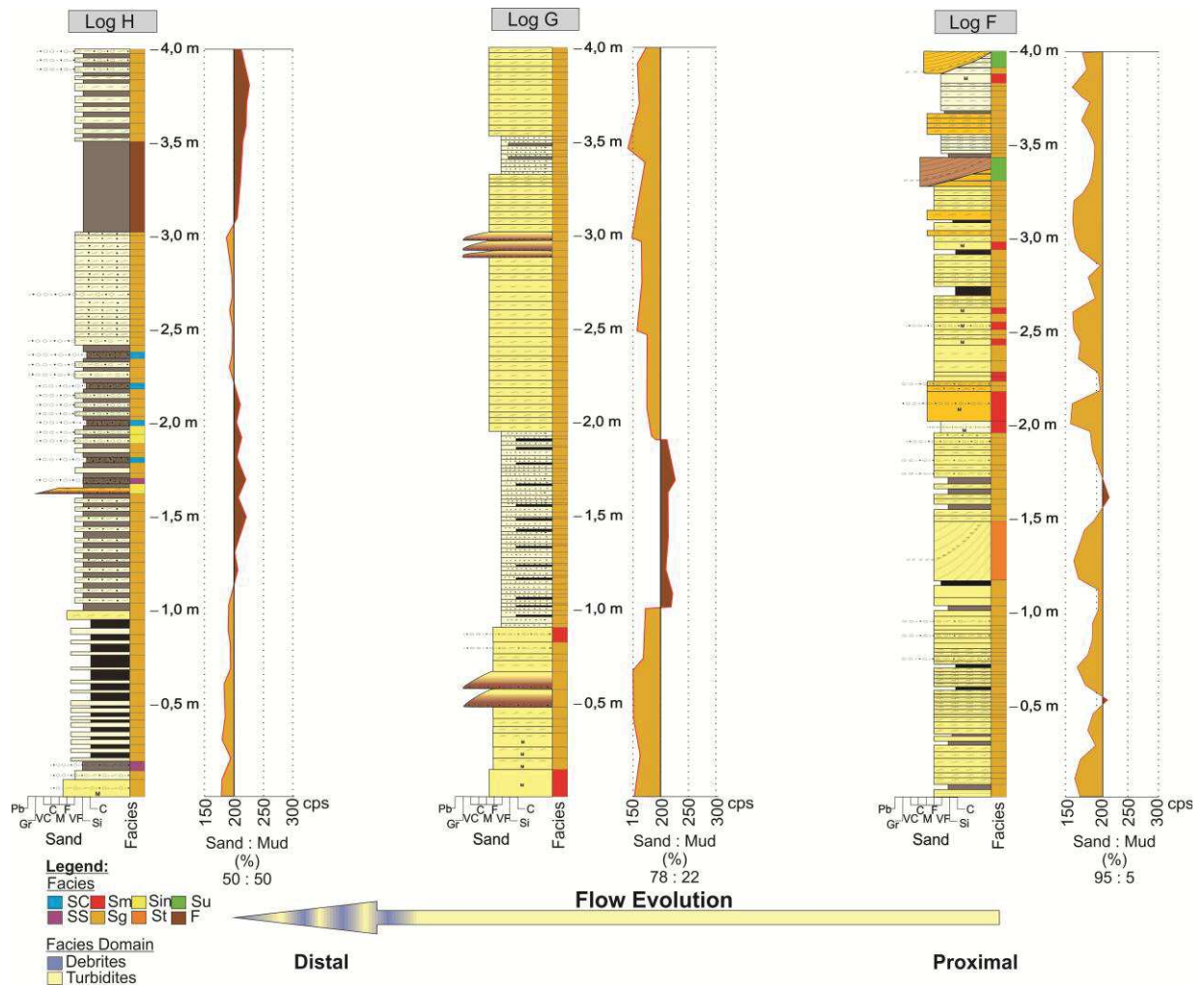


Figure 17 - Facies tracts demonstrated in three sedimentary logs acquired along the highstand system tract. The logs are disposed from the proximal (Log F) through intermediate (Log G) to distal (Log H) reaches.

4.5.2 General Facies Tract

Facies tracts along each depositional system tract are similar and display the same general trends. In terms of sediment gravity flows, all systems tracts contain a higher relative proportion of high-concentration turbidites in the proximal settings. Downslope, these deposits are replaced by low-concentration turbidites and later by debrites, the last ones following the same trend of increasing mud-content basinwards. This sort of change is supposed to represent flow transformations taking place during single depositional events. Unfortunately, the exposure conditions preclude the analysis of individual beds for long distances. Therefore, it is here assumed that changes on the relative proportion of different types of sediment gravity flows deposits stacked in each log represents the same trend within each specific bed.

As formerly proposed (Paim *et al.*, 2000, 2014), the entire depositional system include a braidplain delta fed by a northeastward flowing braided fluvial system that enters into a shallow lacustrine basin. Therefore, it is presumed a tripartite physiography including a flat and horizontal delta plain, whose deposits are preserved elsewhere, and prodelta separated by a gentle, but relatively steeper delta front. Besides, the delta front delineates the gradual transition from channelized flows (braided delta plain and mouth bar) to the unconfined underflows related to the rest of the delta front and prodelta/lacustrine realm (Fig. 13).

5. DISCUSSION

This discussion is based on transport and depositional mechanisms deduced from facies and depositional system specific sub-environments inferred from the facies association. Presumed physiography was deduced from the interpreted depositional systems and theoretical considerations on flow transformation and rheology.

Paleocurrents readings from ripple cross lamination and trough cross bedding (Sg and St facies) related to a proximal delta front setting confirm paleoflows to NE, except by one location (Log I) where paleocurrent mean vector points to south, suggesting the presence of minor lateral input (Fig. 14).

Facies associations include only part of the delta depositional system, more specifically the proximal (facies association 1), intermediate (facies association 2) and distal (facies association 3) delta front to prodelta.

The relative proportion of the turbidites, dominant in the intermediate portions of the delta front, and debrites, increasing towards the distal areas, deserves some further discussion to properly explain the downstream increase on clay content in the sandstone matrix. For instance, the St facies in the proximal areas (facies association 1) shows no mud clast content. However, in the intermediate portions (facies association 2), this facies presents a large amount of mud clasts along its cross-stratification. Other facies (Sg and Sin) are also rich in mud clasts in the intermediate portion. But in the distal areas, where muddy facies and debrites predominate, mud clasts become much rarer (Fig. 18). This trend of mud clasts distribution suggests that mud erosion and its incorporation into the flow takes place in the intermediate portions of the delta front.

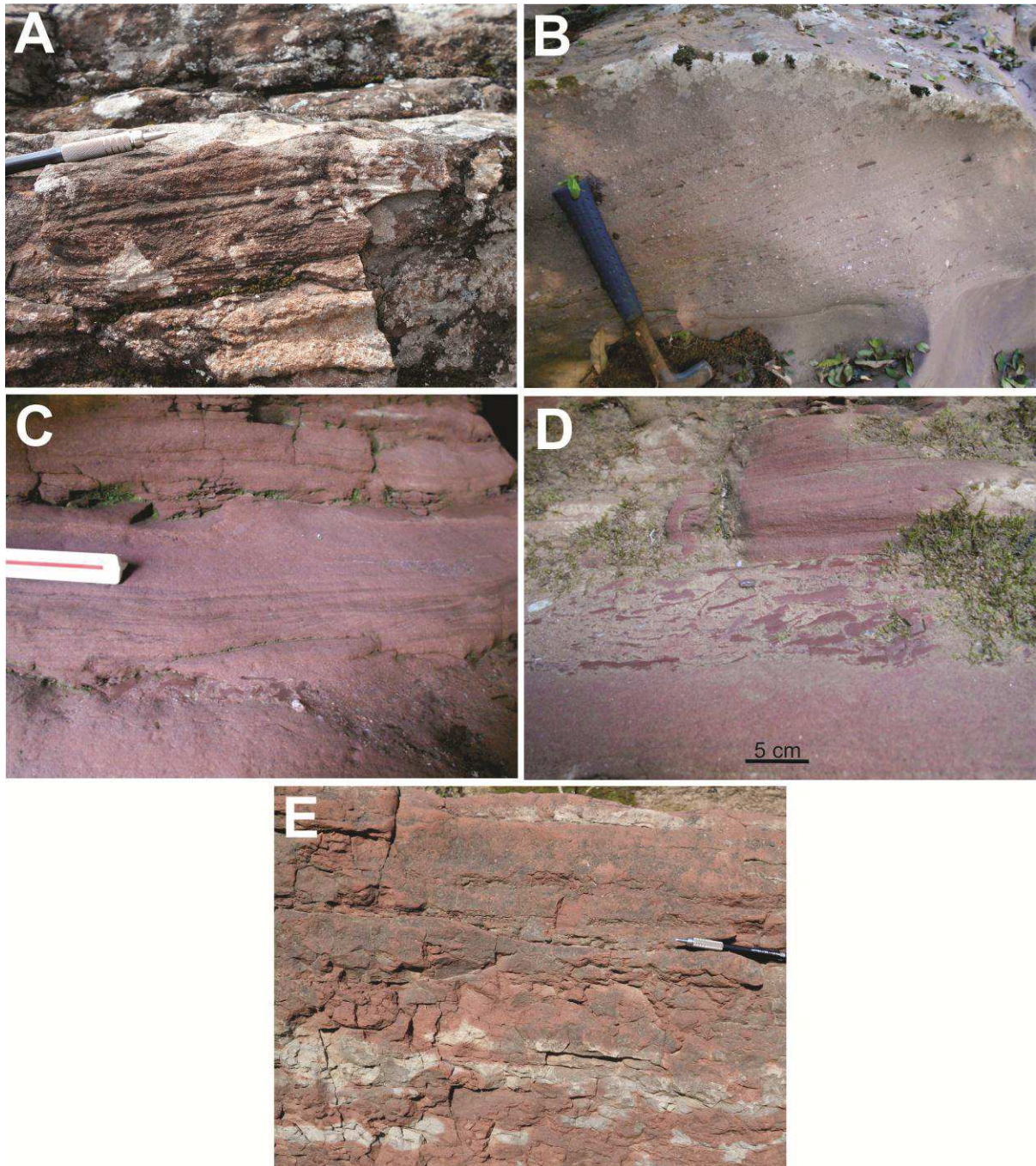


Figure 18 – Changes on the mud clasts content along the delta front: lack and abundance of mud clasts in the St facies recorded in the proximal (A) and intermediate (B) portions of the delta front. Abundant mud clasts in the Sin (C) and Sg (D) facies present in the intermediate portions of the delta front; and E) low content of mud clasts in the distal, mud-rich portions of the delta front.

The only identified clay mineral is vermiculite $(Mg.(Mg,Fe)_3(Si,Al)_4O_{10}(OH)_2 \cdot 4H_2O)$. It has been related to weathering or hydrothermal alteration of biotite and chlorites present in metamorphic and mafic rocks (Mg/Fe-rich) under seasoned climates (Meunier, 2005). The oxidizing environment alters biotite or chlorite (oxidation of Fe^{2+} ions) into dioctahedral vermiculite (Meunier, 2005). Vermiculite may also be related

to the neoformation or degradation of phyllosilicates such as plagioclase through sericite to vermiculite (neoformation). Vermiculite is hydrophilic, or a good electron donor, mainly due the presence of exchangeable ions on the cleavage faces and the capacity of substitution of Al for Si in the cleavage faces, making the oxygen a good electron donor (effective Lewis bases) that creates hydrogen-bonds with water molecules (Chesworth, 2008). Vermiculite ability to cation exchange favors its swelling capacity (Lal & Shukla, 2004). Therefore, vermiculite swelling capacity and cationic bond with the water must increase cohesion of vermiculite-rich debris flows.

Mouth-bar (St) and transitional flow regime (Su) deposits of the most proximal facies association record bedload transport and deposition just beyond the distributary mouths from gradually spreading and thinning underflows along steeper settings. As previously pointed, high-concentration turbidites are often associated with these facies and indicate the formation of denser, basal layers related to bipartite currents derived from the suspended load at the streams mouths. Underflow bi-partition was enhanced by the gradual velocity decrease due to the effluent jet lateral expansion. It is here understood that increase on the concentration near the base of the bipartite turbidity currents has eventually led to the frictional freezing of this basal, laminar layer, and ensuing deposition of massive sandstones (Sm) (Lowe, 1982).

The upper, more diluted layer of the bipartite turbidite current continue to flow downstream towards muddier settings. Its turbulent nature, probably enhanced at the base of the delta front slope, would explain the increase on the mud clast content in the low concentration turbidite beds. Mud clasts are disposed at the base or dispersed within these beds, which often display features related to the increasing fragmentation of the mud clasts (Fig. 19) and resulting increase on the mud content in the flow. The idea of a genetic relationship between low concentration turbidity currents and debris flow is also supported by the fact that the grain size population of both is identical, except by the larger mud content in the debrites. This process culminates with the transformation of a turbulent current into a cohesive debris flow. As a result, low-density turbidite current deposits (Sg, Sin) dominate the intermediate portions of the delta front (facies association 2) whereas debris flow facies (SC and SS) became more abundant towards the distal delta front to prodelta realm (facies association 3).

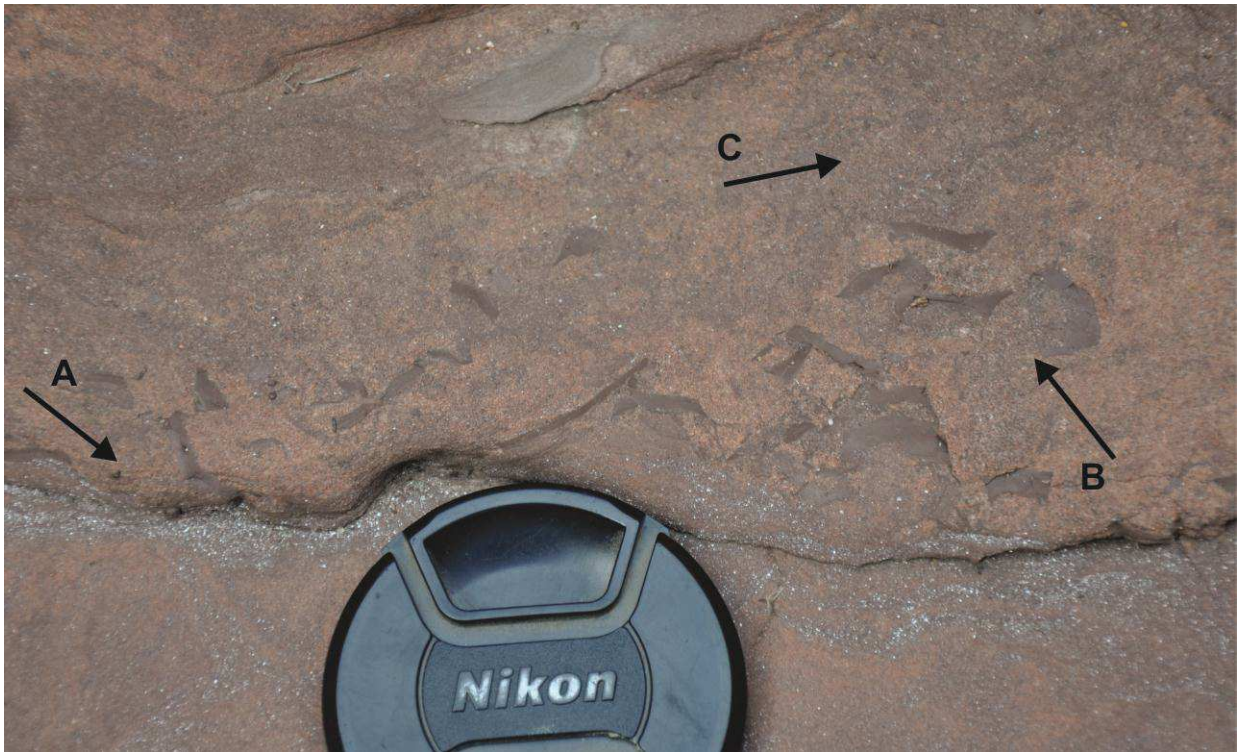


Figure 19 – Incorporation of clay into turbidite facies: erosion of a lower muddy layer producing mud clasts (A) that are progressively crushed (B) and turned into a clayey depositional matrix (C).

The association between turbidites and linked debrites has been explained in different ways (Talling *et al.*, 2004, 2007; Baas *et al.*, 2009, 2011; Haughton *et al.*, 2009):

1. An initial turbidity current erodes the basin floor, causing flow bulking and transformation into a debris flow;
2. An initial debris flow is diluted by shear with the ambient fluid, producing a turbidity current that outruns the debris flow;
3. An initial turbidity current may generate a secondary debris flow by loading an unstable substrate;
4. Turbidity current deceleration may be accompanied by an abrupt transition from turbulent to laminar flow;
5. A debris flow with low strength decelerates and particles above a critical size settle out, whereas the smaller particles remain suspended in the flow, generating turbidity current.

The first hypothesis above indicated is then used to explain the change from low-concentration turbidites into debrites. It is worth to notice that several authors have explained the increase of clay matrix by erosion, fragmentation and disaggregation of mud clasts by the precursor turbidity current (Talling *et al.*, 2004, 2012; Amy & Talling, 2006; Haughton *et al.*, 2009; Sumner *et al.*, 2009; Southern *et al.*, 2016). At last, and like hypothesis 2, a diluted plume developed along the upper layer of the debris flow due to water incorporation and stripping of surface materials produces a finer-grained, low

concentration plume deposited above the debrites as a thin turbidite layer, thus forming hybrid beds similarly to the model proposed by Talling *et al.* (2012) to explain the deposition of hybrid beds with debrite at the base and turbidites on top (Fig. 20).

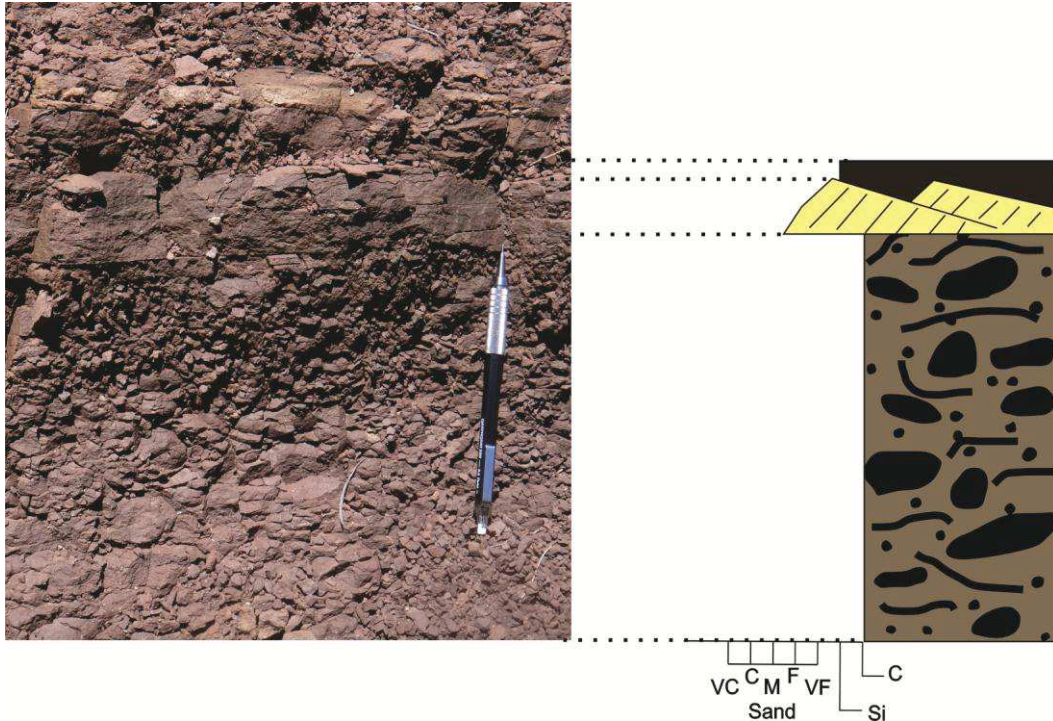


Figure 20 – Outcrop photograph in the studied area and graphic representation of hybrid bed; debrite on the base, sandy turbidite with ripple-cross lamination on top and thin mud cap (Modified from Talling *et al.*, 2012).

Figure 21 summarizes the above mentioned ideas as an idealized depositional model that explains the downdip facies tract in terms of three subsequent types of flow transformations (Fisher, 1983): (1) gravity flow transformation, when the initial underflow decelerate and becomes a high-concentration turbidity current; (2) body flow transformation, when the turbidity current change to a debris flow by mud incorporation; and (3) surface flow transformation, when the debris flow deposits and the dilution plume continue flowing. The increasing clay mineral content in the matrix, in special vermiculite, is supposed to have played an important role on the transformation of the turbidity currents into debris flows.

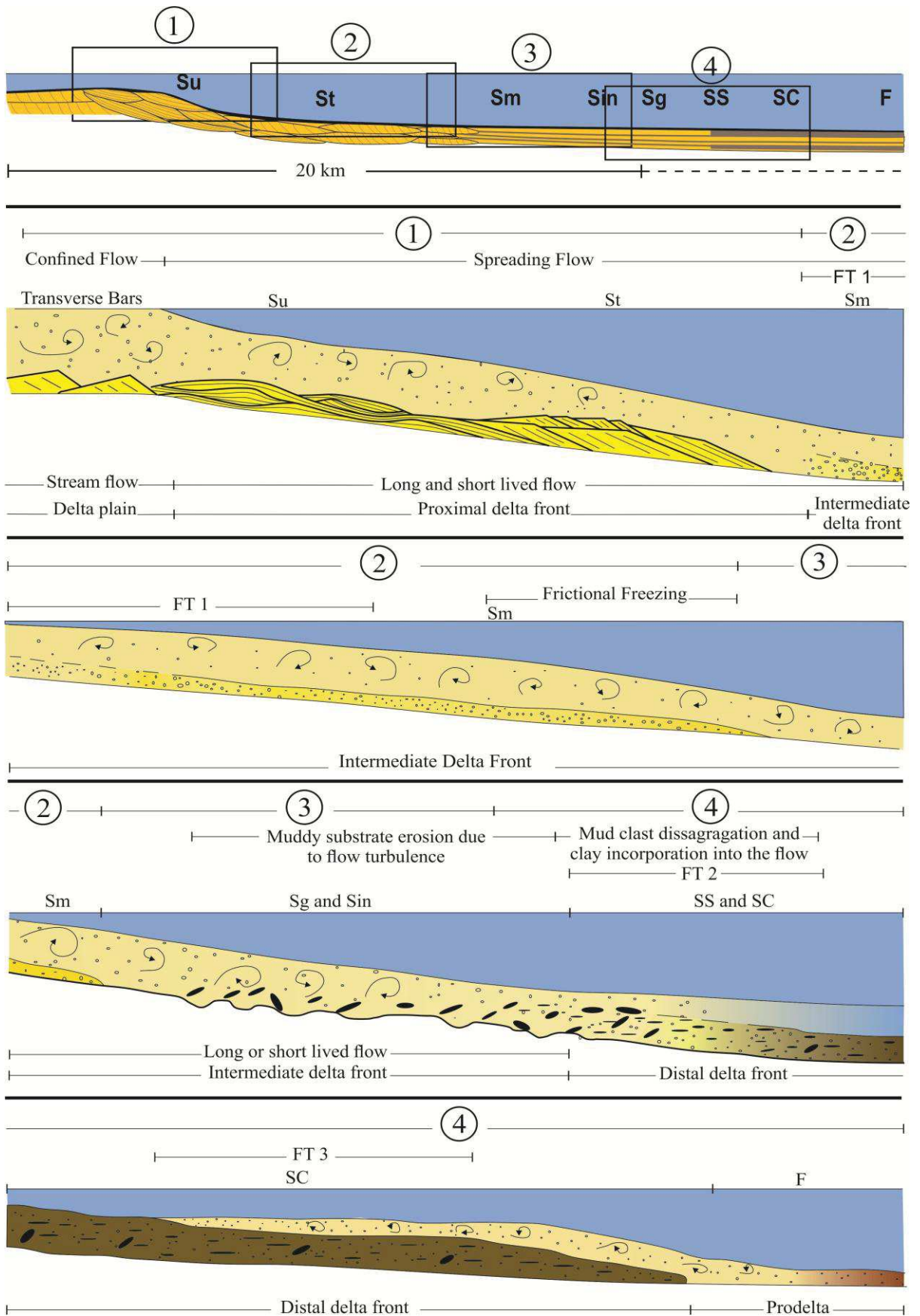


Figure 21 – Facies tract and flow evolution model. From 1 to 4: stream flow at the mouth bar, bipartite flow, high and low-concentration turbidity currents, mud incorporation and transformation into a debris flow and deposition of the turbidity plume derived from the dilution of the upper part of the debris flow.

6. CONCLUSIONS

The Serra dos Lanceiros Alloformation comprises delta and lacustrine deposits that includes sediment gravity flows deposition. Eventual large scale lake-level fluctuations are recorded by sporadic mud cracks within distal mudstones. Sediment-laden effluents are indicated by the abundance of fluvial-derived sediment gravity flows.

Facies tract indicates flow transformations and hybrid flows. First of all, the distributary channel bedload is released at their mouths and their suspended load detaches as a underflow. The first flow transformation occurs when this underflow gradually spreads and consequently decelerates, generating bipartite turbidity currents with a basal, laminar denser layer. The second flow transformation occurs when the low concentration turbidity current detaches from the denser, now frozen basal layer and erodes the substrate, incorporating mud and producing cohesive debris flows. And the last flow transformation takes place when a low concentration plume is produced at the top of the debris flow depositing a thin turbidity layer above the debris.

Change from fluidal to plastic flow rheology was caused by substrate erosion, and incorporation and fragmentation of mud clasts by turbulent flows. XRD and SEM analyses indicated vermiculite as the clay mineral present in the rock matrix. Vermiculite exchangeable cation nature and swelling capacity enhanced cohesive strength of the matrix.

Short- and long-lived turbidity currents are recorded. Taking into account the proximal to distal facies relationships, it seems logical to associate turbidity currents with fluvial floods. The presence of both graded (Sg) and inverse-to-normal graded (Sin) turbidite facies suggests triggering of the turbidity currents caused either by the direct fluvial input (hyperpycnal flows) or by multiple retrogressive failures of sand bars at river mouth during flood events (Mulder & Alexander, 2001).

7. ACKNOWLEDGEMENTS

The first author thanks CAPES for providing a scholarship, Petrobras for financial support, MSc. Garibaldi Armelenti and MSc. Marinez Oliveira for the assistance with petrography and Dr. Farid Chemale Jr, Dr. Andrea Sander and Dr. Cassiana Michelin for the assistance with X-Ray and SEM analyses. The authors recognize Universidade do Vale do Rio dos Sinos (Unisinos) for providing lab facilities and field equipments. The last author thanks CNPq for long lasting research support.

8. REFERENCES

- Allen, J. P., Fielding, C. R., Gibling, M. R., Rygel, M. C., 2014. Recognizing products of palaeoclimate fluctuation in the fluvial stratigraphic record: An example from the Pennsylvanian to Lower Permian of Cape Breton Island, Nova Scotia. *Sedimentology*, 61: 1332–1381;
- Almeida, F., 1969. Diferenciação Tectônica da Plataforma Brasileira. In: Congr. Bras. Geol., 1, Salvador, pp. 29-46; Almeida, F.; Hasui, Y.; Brito Neves, B., 1976. The Upper Precambrian of South America. *Boletim IG/USP*, Vol.7, pp.45-80;
- Almeida, F., Hasui, Y., Brito Neves, B., Fuck R., 1981. Brazilian structural provinces: an introduction. *Earth Science Ver*, Vol.17, pp.1-29;
- Almeida, R.P., 2001. Evolução Tectono-Sedimentar da Formação Santa Bárbara na Bacia do Camaquã Ocidental. Dissertação de Mestrado, USP, São Paulo;
- Amy, L.A. & Talling, P.J., 2006. Anatomy of turbidites and linked debrites based on long distance (120 x 30 km) bed correlation, Marmoso Arenacea Formation, Northern Apennines, Italy. *Sedimentology*, 53, 161-212;
- Baas, J.H., Best, J.L., Peakall, J., Wang, M., 2009. A phase diagram for turbulent, transitional and laminar clay suspension flows. *J. Sed. Res.*, 79, 162-183;
- Baas, J.H., Best, J.L., Peakall, J., 2011. Depositional processes, bed form development and hybrid bed formation in rapidly decelerated cohesive (mud–sand) sediment flows. *Sedimentology*, 58, 1953-1987;
- Bates, C.C., 1953. Rational Theory of Delta Formation. *Bulletin of the American Association of Petroleum Geologists*. Vol.3, n° 9. PP. 2119-2162;
- Borba, A.W. & Mizusaki, A. M. P., 2003. Santa Bárbara Formation (Caçapava do Sul, southern Brazil): depositional sequences and evolution of an Early Paleozoic post-colisional basin. *Journal of South American Earth Sciences*. Grã-Bretanha: v.16, n.5, p.365 – 380;
- Bouma, A.H., 1962. *Sedimentology of Some Flysch Deposits: a Graphic Approach to Facies Interpretation*: Amsterdam, Elsevier, 168p;
- Caineng, Z., Lan, W., Ying, L., Shizhen, T., Lianhua, H., 2012. Deep-lacustrine transformation of sandy debrites into turbidites, Upper Triassic, Central China. *Sedimentary Geology*, 265, 143-155;
- Chemale Jr., F., 2000. Evolução geológica do Escudo Sul-riograndense, in: HOLZ, M.; DE ROS, L.F. (Eds), *Geologia do RS*. CIGO/UFRGS, Porto Alegre, pp. 13-52;
- Chemale Jr., F.; Hartmann, L.A.; Silva, L.C., 1995. Stratigraphic and tectonism of Precambrian to Early Paleozoic units. *XVIII Acta Geologica Leopoldensia*, 42, 5-117;

- Chesworth, W., 2008. Encyclopedia of soil science. Springer, Canada. 860 p;
- CPRM, 1995. Passo do Salsinho, Folha SH.22.Y.A.I-4 – Estado do Rio Grande do Sul, Escala 1:50.000. Brasília, 1995;
- Dott, R.J. & Bourgeois, J., 1982. Hummocky stratification: significance of its variable bedding sequences. Geological Society of America Bulletin 93, 663–680;
- Fallgatter, C., Kneller, B., Paim, P. S. G., Milana, J. P., 2016. Transformation, partitioning and flow–deposit interactions during the run-out of megaflores. Sedimentology;
- Fielding, C.R., 2006, Upper flow regime sheets, lenses and scour fills: extending the range of architectural elements for fluvial sediment bodies: Sedimentary Geology, v. 190, p. 227–240;
- FISHER, R. V., 1983. Flow transformations in sediment gravity flows. Geology, v.11, p. 273-274;
- Fragoso-César, A. R., Fambrini, G., Paes de Almeida, R., Pelosi, A., Janikian, L., Riccomini, C., Machado, R., Nogueira, A., Saes, G., 2000. The Camaquã extensional basin: Neoproterozoic to early Cambrian sequences in Southernmost Brazil, Revista Brasileira de Geociências, Vol.30, pp.438-441, ISSN 0375-7536;
- Fragoso-César, A.R.S., Lavina, E.L., Paim, P.S.G., Faccini, U.F., 1984. A antefossa molássica do Cinturão Dom Feliciano no Escudo do Rio Grande do Sul. In: Congresso Brasileiro de Geologia, 33, 3272-3283;
- Fonnesu, M., Haughton, P.D.W., Felletti, F., and McCaffrey, W.D, 2015.Short-length scale variability of hybrid event beds and its applied significance. Marine and Petroleum Geology 67, 583-603.
- Girard, F., Ghienne, J. F., Rubino, J. L., 2012. Occurrence of hyperpicnal flows and hybrid event beds related to glacial outburst events in a late Ordovician proglacial delta (Murzuq basin, SW Libya). *J. Sed. Res.*, 82:688-708;
- Hartmann, L. A.; Santos, J. O. S. ; McNaughton, N. J., 2008. Detrital zircon U-Pb age data, and Precambrian provenance of the Paleozoic Guaritas Formation, southern Brazilian Shield. International Geology Review , v. 50, p. 364-374;
- Harms, J.C., Southard, J.B., Walker, R.G., 1982. Structures and sequences in clastic rocks. Society for Sedimentary Geology (SEPM) Short Course, 9 (249 pp.);
- Haughton, P., Davis, C.; McCaffrey, W.; Barker, S., 2009. Hybrid sediment gravity flow deposits – classification, origin and significance. Marine and Petroleum Geology, v. 26, p. 1900-1918;
- Janikian, L., De Almeida, R.P., Fragoso-César, A.R.S., Martins, V.T.D.S., Dantas, E.L., McReath, I., D'Agrella-Filho, M.S., 2012. Ages (U-Pb SHRIMP and LA ICPMS) and stratigraphic evolution of the Neoproterozoic volcano-sedimentary successions from the extensional Camaquã Basin, Southern Brazil .Gondwana Research 21, 466-482;
- Justo, A.P. & Almeida, R.P., 2004. Controles tectônicos e influência do soerguimento do Alto de Caçapava do Sul na sedimentação do Grupo Santa Bárbara (Eopaleozóico, Bacia do Camaquã). In: Cong. Bras. Geol., 42, Araxá, MG, Anais. v. S02. p. 348;
- Lal, R. & Shukla, M.K., 2004. Principles of Soil Science. Marcel Dekker Inc., New York, 699p.;
- Leeder, M. R., 1999. Sedimentology and Sedimentary Basins: from Turbulence to Tectonics. Blackwell Science, Oxford;
- Lowe, D.R., 1982. Sediment gravity flows II: Depositional models with special reference to the deposits of high-density turbidity currents. J. Sed. Petrol., 52, 279-297;
- Lowe, D.R. & Guy, M., 2000. Slurry-flow deposits in the Britannia Formation (Lower Cretaceous), North Sea: a new perspective on the turbidity current and debris flow problem. Sedimentology, 47, 31–70;

- Meunier, A., 2005. *Clays*. Springer Berlin Heidelberg. Germany. 472 p.;
- Middleton, G. V. & Hampton, M. 1973. Sediment gravity flows: mechanics of flow and deposition In: G. V. Middleton & A. Bouma (eds.). *Turbidites and deep water sedimentation*. Los Angeles, SEPM (Pacific Section) Short Course 1, Anaheim. 1973. Lecture Notes. p. 1 – 38;
- Morad, S., 1998. Carbonate cementation in sandstones: distribution patterns and geochemical evolution. *Spec. Publs Int. Ass. Sediment.* 26, 1-26;
- Morad, S., Al-Ramadan, K., Ketzer, J. M. & De Ros, L. F., 2010. The impact of diagenesis on the heterogeneity of sandstone reservoirs: A review of the role of depositional facies and sequence stratigraphy. *American Association of Petroleum Geologists Bulletin*, 94(8), 1267-1309;
- Mulder, T. & Alexander, J., 2001. The physical character of subaqueous sedimentary density flows and their deposits. *Sedimentology*, 48, 269–300;
- Mulder, T. & Syvitski, J. P.M., 1995. Turbidity currents generated at river mouths during exceptional discharges to the world oceans. *Journal of Geology*, 103, 285–299;
- Mulder, T., Syvitski, J.P.M., Migeon, S., Faugères, J.C., Savoye, B., 2003. Marine hyperpycnal flows: initiation, behavior and related deposits, a review: *Marine and Petroleum Geology*, v. 20, p. 861–882;
- Mutti, E., 1992. *Turbidite sandstones*. San Donato Milanese: AGIP - Istituto di Geologia, Università di Parma, p. 275;
- Mutti, E., Davoli, G., Tinterri, R., Zavala, C., 1996, The importance of fluvio-deltaic systems dominated by catastrophic flooding in tectonically active basins: *Memorie di Scienze Geologiche, Università di Padova*, v. 48, p. 233-291;
- Mutti, E., Tinterri, R., Di Biase, D., Fava, L., Mavilla, N., Angella, S., Calabrese, L., 2000. Delta-front facies associations of ancient flood dominated fluvio-deltaic systems. *Review of the Society of Geology Espana*, 13(2), 165–190;
- Mutti, E., Tinterri, R., Benevelli, G., Di Biase, D., Cavanna, G., 2003. Deltaic, mixed and turbidite sedimentation of ancient foreland basins. *Mar. Pet. Geol.* 20, 733e755;
- Nemec, W. and Steel, R.J., 1984. Alluvial and coastal conglomerates: their significant features and some comments on gravelly mass-flow deposits. In: E.H. Koster and R.J. Steel (Editors), *Sedimentology of Gravels and Conglomerates*. *Mem. Can. Soc. Pet. Geol.*, 10: 1-31.
- Paim, P.S.G., 1994. *Depositional systems and paleogeographical evolution of the Camaquã and Santa Bárbara Basins, Brazil*. Phil. Doctor Thesis, Oxford. v.I, 277 p.;
- Paim, P.S.G., Chemale Jr., F., Lopes, R.C., 2000. A Bacia do Camaquã. In: Holz, M. & De Ros, L.F. (eds.). *Geologia do Rio Grande do Sul*, Porto Alegre, CIGO/UFRGS, p. 231-274;
- Paim, P.S.G., Wildner, W., Chemale Jr., F., 2014. Estágios evolutivos da Bacia do Camaquã (RS). *Ciência e Natura*, Santa Maria, v. 36;
- Ricci Lucchi, F., Valmori, E., 1980. Basin-wide turbidites in a Miocene, over-supplied deep-sea plain: a geometrical analysis. *Sedimentology* 27, 241–270;
- Sanders, J.E., 1965. Primary sedimentary structures formed by turbidity currents and related re-sedimentation mechanisms. In: G.V. Middleton (Editor), *Primary sedimentary structures and their hydrodynamic interpretation*. *Soc. Econ. Paleontol. Mineral., Sprc. Publ.*, 12: 192-217;
- Schultz, J.L., Boles, J.R., Tilton, G.R., 1989. Tracking calcium in the San Joaquin basin, California: a strontium isotopic study of carbonate cements at North Coles Levee. *Geochim. Cosmochim. Acta*, 53, 1991 -1999;

- Shanmugan, G., 1996. High-density turbidity currents: are they sandy debris flows? *Journal of Sedimentary Research*, v. 66, p 2-10;
- Silveira, D.M., 2016. Debritos e Turbiditos na Bacia do Camaquã: depósitos conegéticos ou independentes? Dissertação de Mestrado. UNISINOS, São Leopoldo/RS;
- Sommer, C. A., Lima, E.F., Nardi, L.V.S., Figueiredo, A.M.G., Pierosan, R., 2005. Potassium and low- and high-Ti mildly alkaline volcanism in the Neoproterozoic Ramada Plateau, southernmost Brazil. *Journal of South American Earth Sciences* 18 (3), 237-254;
- Southern, S. J., Kane, I. A., Warchol, M. J., Porten, K. W., McCaffrey, W. D., 2016. Hybrid event beds dominated by transitional-flow facies: Character, distribution and significance in the Maastrichtian Springar Formation, north-west Vøring Basin, Norwegian Sea. *Sedimentology*. Accepted Article;
- Sumner, E.J., Talling, P.J., Amy, L.A., 2009. Deposits of flows transitional between turbidity current and debris flow: *Geology*, 37, 991-994;
- Takahashi, T., 1981. Debris Flow. *Annu. Rev. Fluid Mech.*, 13, 57-77;
- Talling, P.J., Amy, L.A., Wynn, R.B., Peakall, J., Robinson, M., 2004. Beds comprising debrite sandwiched within co-genetic turbidite: origin and widespread occurrence in distal depositional environments. *Sedimentology*, 51, 163-194;
- Talling, P.J., Wynn, R.B., Masson, D.G., Frenz, M., Cronin, B.T., Schiebel, R., Akhmetzhanov, A.M., Dallmeier-Tiessen, S., Benetti, S., Weaver, P.P.E., Georgiopoulou, A., Zülsdorff, C., Amy, L.A., 2007. Onset of submarine debris flow deposition far from original giant landslide. *Nature*, 450, 541-544;
- Talling, P.J., Malgenisi, G., Sumner, E.J., Amy, L.A., Felletti, F., Blackbourn, G., Nutt, C., Wilcox, C., Harding, I.C., Akbari, S., 2012. Planform geometry, stacking pattern, and extrabasinal origin of low strength and intermediate strength cohesive debris flow deposits in the Marnoso-arenacea Formation, Italy. *Geosphere* 8 (6), 1207e1230;
- Talling, P.J., Masson, D.G., Sumner, E.J., Malgesini, G., 2012. Subaqueous sediment density flows: Depositional processes and deposit types. *Sedimentology*, 59, 1937-2003;
- Tinterri, R., Drago, M., Consonni, A., Davoli, G., Mutti, E., 2003. Modelling subaqueous bipartite sediment gravity flows on the basis of outcrop constraints: first results. *Marine and Petroleum Geology* 20, 911–933;
- Tucker, M.E., 2001. *Sedimentary Petrology* (3rd ed.). Blackwell Science, Osney Mead, Oxford OX2 0EL, UK; 262 p.;
- Ulmer-Scholle, D. S.; Scholle, P. A.; Schieber, J.; Raine, R. J., 2014. A color guide to the petrography of sandstones, siltstones, shales and associated rocks;
- Walker, T.R., 1976. Diagenetic origin of continental red beds. Pp. 240-282. In: *The Continental Permian in Central, West, and South Europe* (H. Falke, editor). D. Reidel Publishing Company, Dordrecht, The Netherlands;
- Walker, R.G., 1978. Deep-water sandstone facies and ancient submarine fans – models for exploration and for stratigraphic traps. *AAPG Bull.*, 62, 932–966;
- Walker, R.G., Duke, W.L., Leckie, D.A., 1983. Hummocky stratification: significance of its variable bedding sequences: discussion and reply. *Geological Society of America Bulletin* 94, 1245–1251;
- Wheatcroft, R.A., 2000. Oceanic flood sedimentation: a new perspective. *Cont. Shelf Res.* 20, 2059-2066;

- Wright, L.D., 1977. Sediment transport and deposition at river mouths: A synthesis. Geological Society of America Bulletin, v. 88, p. 857-868;
- Worden, R.H. & Morad, S., 2000. Quartz cementation in oil field sandstones: a review of the key controversies. In: Quartz cementation in sandstones. Worden, R.H. & Morad, S (Edit.). Spec. Publs Int. Ass. Sediment. 26, 1-26;
- Wright, L.D., Wiseman, W.J., Prior, D.B., Suhayda, J.N., Keller, G.H., Yang, Z.-S., Fan, Y.B., 1988. Marine dispersal and deposition of Yellow River silts by gravity driven underflows. Nature, 332, 629-632;
- Zavala, C., Ponce, J.J., Arcuri, M., Drittanti, D., Freije, H., and Asensio, M., 2006. Ancient lacustrine hyperpycnites: a depositional model from a case study in the Rayoso Formation (Cretaceous) of west-central Argentina: Journal of Sedimentary Research, v. 76, p. 41–59.

SÍNTESE FINAL

Dentre os resultados discutidos e interpretados no manuscrito ficam destacados os apontamentos sobre as transformações de fluxo registradas nos depósitos de fluxos gravitacionais de sedimentos presentes do intervalo de estudo.

Essa pesquisa investigou com detalhe os depósitos de fluxos gravitacionais de sedimentos identificados na sequência deposicional estudada. Ferramentas como a fotointerpretação, levantamento de perfis estratigráficos e gama e o reconhecimento de afloramentos, foram utilizadas para identificação e descrição de oito fácies sedimentares. A presença de argila nos depósitos de debritos e turbiditos, indicando um componente de coesão para os fluxos, foi averiguada através de análise petrográfica, MEV e Raio X. As análises realizadas indicaram a presença de vermiculita, uma argila bastante coesiva, devido às suas propriedades físico-químicas.

O refinamento estratigráfico da área, realizado com o intuito de posicionar os afloramentos em um arcabouço genético, permitiu o reconhecimento de novas superfícies estratigráficas, sendo definidas três sequências deposicionais para a área. Das três sequências, a intermediária apresenta os melhores afloramentos. Dessa forma, foram analisadas as fácies, associações de fácies e trato de fácies no interior da sequência escolhida. As fácies foram agrupadas nas associações de fácies 1, 2 e 3 que representam as porções proximais, intermediárias e distais da frente deltaica, respectivamente.

Os perfis levantados nas porções proximais, intermediárias e distais dentro dos tratos de sistemas de nível baixo, transgressivo e de nível alto, apresentaram um padrão deposicional que se repete. Dessa forma, a espacialização das fácies dentro do trato de fácies inclui desde fácies de barras de desembocadura de distributários deltaicos e de regime de fluxo transicional, passando para turbiditos de alta concentração, turbiditos de baixa concentração, debritos, camadas híbridas e, por fim, sedimentação fina lacustre. Foram propostas três transformações de fluxos: uma primeira, por gravidade, quando o fluxo desconfinado, se expande e desacelera, tornando-se uma corrente de turbidez bipartida; uma segunda, de corpo, que ocorre quando a corrente de turbidez de baixa concentração, que se descolou da de alta concentração quando essa congelou, erode e incorpora argila do substrato, torna-se um fluxo de detritos coesivo; e uma última, de superfície, quando uma pluma turbulenta de sedimentos finos em suspensão se forma na porção superior do fluxo de detritos devido a incorporação de água ambiente

A relação física entre depósitos de fluxos hiperpicnais e turbiditos de baixa concentração, somada à relação lateral de dessas fácies com depósitos de barras de desembocadura, indica que tanto as correntes de turbidez de longa (*quasi-steady*) como de curta (*surge*) duração estejam relacionada a cheias fluviais.

A pesquisa abordou apenas um intervalo de uma unidade da Bacia do Camaquã. Entende-se que para uma melhor compreensão dos fenômenos abordados, o trabalho deva

ser ampliado para as demais unidades. No entanto, para dirimir dúvidas acerca da correlação dos distintos blocos estruturais da Bacia do Camaquã, uma abordagem mais ampla, respaldada por um extenso trabalho de geocronologia, deveria ser associada à estratigrafia, sedimentologia e petrologia.